

Volcano deformation analysis in the Lazufre area (central Andes) using geodetic and geological observations

**Dissertation zur Erlangung des akademischen Grades "doctor rerum naturalium"
(Dr. rer. nat.) in der Wissenschaftsdisziplin "geologie"**

**eingereicht an der
Mathematisch-Naturwissenschaftlichen Fakultät
der Universität Potsdam**

von Joël Ruch

Published online at the
Institutional Repository of the University of Potsdam:
URL <http://opus.kobv.de/ubp/volltexte/2010/4736/>
URN <urn:nbn:de:kobv:517-opus-47361>
<http://nbn-resolving.org/urn:nbn:de:kobv:517-opus-47361>

I herewith declare that I have produced this paper without the prohibited assistance of third parties and without making use of aids other than those specified; notions taken over directly or indirectly from other sources have been identified as such. This paper has not previously been presented in identical or similar form to any other German or foreign examination board. This work has been financially supported by the German Research Foundation (DFG) through the grant #WA1642 and the GFZ German Centre for Geosciences.

Potsdam, 28.01.2010

Joel Ruch

Un voyage ne commence pas au moment où l'on se met en route et ne se termine pas lorsque l'on arrive à destination. En réalité, il débute bien plus tôt et ne s'arrête pratiquement jamais.

Ryszard Kapuściński

Acknowledgements

During three years I spend at GFZ I met people from Germany but also from different countries with diverse cultural and scientific backgrounds and this was one of the strength of this period. I would like first to thank my supervisor Thomas Walter that provides me the opportunity to work in his group, I learned a lot during this period, from both scientific and personal point of view. I thank all the people from section 2.1 for good moments we spend together at GFZ and during short coffee break, in particular “reingrazio” my italian friends, Matteo, Angelo and Domenico, with who I spend three warm years speaking about this far Italy that I am now discovering. I also thank Silke and Simone that take care of my dog during frequent travel to Italy, or during field work, and for very tasty dinners we shared accompanied of good wines! Then I thank colleagues of my ex-office, Manoochehr, Hannes and Ane, we who I shared good moments. As I spend a total of three month in field mission installing and testing instruments at volcanoes, I would like to thank people with who I worked during mission preparation and fieldwork, first the technicians, H. Pflug, E. Gunther and especially Hermann Loeper, that had always the perfect solution in mind for instrument constructions and realizations, I think our section will miss him since he retired. I thank then Birger for great moments shared in the field, that gave me some tricks for driving in the Andean desert hearing “Black girl”, Heiko with who I installed my first seismic station on a hotel terrace in Dominica, briefly after a M7 earthquake. Nicolas Fournier for great fieldworks we spend together, he showed me the basics for using (or not!) a “gravimata” in all conditions, then I thank le breton Nicolas Le Corvec for good dinners

he prepared during transient collocation and his inestimable help at 5400 asl drilling holes for GPS measurements, I also thank Jean-Luc Froger and Philippe Labazuy for hard but pleasant moments we spend during a week at Lazufre at -15C at night and at the Lastarria summit, then come people from the University of Antofagasta (UCN), the Prof. Medina and his students that helped us with an incredible motivation in the field in really harsh conditions, Felipe Aguilera for good memories when sampling and inhaling gases at the Isluga and Lastarria volcanoes. I would like then really to thank Andrea, compaignon de route, who beside having been helpful for learning Italian and matlab basics, we share many great moment during three years “face a face” in the office, on the field and elsewhere in Berlin. All my gratitude go then to my parents in Geneva, Grisons, and also Ursula from Bienne, that sustained me during these three years with pleasant messages. I would like finally to address all my love to Sarah, that encourages me in all important choices I took, going in other continents to speak with these far volcanoes, and who sustained me during stressful period. Sorry for these long “silence radio” during field work! She is the one that arrives to create from any single and simple moment in life a great atmosphere.

Table of contents:

ABSTRACT	10
ZUSAMMENFASSUNG	11
CHAPTER 1	13
INTRODUCTION	13
1.1 GOALS AND MOTIVATION	13
1.2 VOLCANO-TECTONIC RELATIONSHIP	14
1.3 LARGE-SCALE VOLCANO DEFORMATION	14
1.4 METHODS USED	15
1.4.1 Remote sensing observations	15
1.4.2 Field observations at Lazufre	16
1.4.3 Modeling surface deformation	18
1.5 THESIS ORGANISATION	18
1.5.1 Caldera-scale inflation of the Lazufre volcanic area, South America: evidence from InSAR	19
1.5.2 Stress transfer in the Lazufre volcanic area, central Andes	19
1.5.3 Short-term and long-term volcano deformations as potential stress field indicator in the central Andes	20
1.5.4 Deforming salars as a potential tool for monitoring environmental change	20
CHAPTER 2	23
CALDERA-SCALE INFLATION OF THE LAZUFRE VOLCANIC AREA, SOUTH AMERICA: EVIDENCE FROM INSAR .	23
ABSTRACT	23
2.1 INTRODUCTION	24
2.2 THE 2003 – 2006 DEFORMATION	26
2.2.1 InSAR data	26
2.2.2 Volume and area increase	28
2.2.3 Source modelling	29
2.3 DISCUSSION	32
2.3.1 Limitations of the models	33
2.3.2 Multiple source evidence	34
2.3.3 The comparison to other inflation caldera systems	34
2.3.4 Source origin	36
2.3.5 Earthquake triggering of magma intrusion	37
2.3.6 Total volume of the source	37
2.4 CONCLUSION	39
2.5 ACKNOWLEDGEMENTS	39
CHAPTER 3	41
STRESS TRANSFER IN THE LAZUFRE VOLCANIC AREA, CENTRAL ANDES	41
ABSTRACT	41
3.1 INTRODUCTION	42
3.2 DEFORMATION MEASUREMENTS	44
3.3 SOURCE MODELING	45
3.4 DEFORMATION STARTS AND STRESS TRANSFER MODELING	47
3.5 DISCUSSION AND CONCLUSIONS	50

3.6 ACKNOWLEDGEMENTS	52
3.7 AUXILLIARY MATERIAL	52
CHAPTER 4.....	57
RELATIONSHIP BETWEEN CURRENT UPLIFT GEOMETRY (INSAR) AND THE STRUCTURAL FRAMEWORK AT LAZUFRE VOLCANIC AREA, CENTRAL ANDES	57
ABSTRACT	57
4.1 INTRODUCTION	58
4.1.1 <i>Volcano-tectonic context</i>	60
4.2 RECENT DEFORMATION AND STRUCTURAL FRAMEWORK ANALYSIS	61
4.2.1 <i>Deformation geometry detected by InSAR</i>	62
4.2.2 <i>Volcanic structures analysis</i>	63
4.2.3 <i>Volcano lineament and volcano deformation as stress field indicators</i>	65
4.3 DISCUSSION	67
4.4 CONCLUSION	70
4.5 ACKNOWLEDGEMENTS	70
CHAPTER 5.....	73
SALT LAKE GROWTH DETECTED FROM SPACE	73
ABSTRACT	73
5.1 CLIMATIC AND SEDIMENTOLOGIC FRAMEWORK.....	74
5.2 DEFORMATION MEASUREMENTS	76
5.3 DEFORMATION SIGNAL VERSUS GROUND COMPOSITION	80
5.4 DISCUSSION & CONCLUSION	81
CONCLUSION AND OUTLOOK	85
REFERENCES.....	88
CURRICULUM VITAE.....	97

Abstract

Large-scale volcanic deformation recently detected by radar interferometry (InSAR) provides new information and thus new scientific challenges for understanding volcano-tectonic activity and magmatic systems. The destabilization of such a system at depth noticeably affects the surrounding environment through magma injection, ground displacement and volcanic eruptions. To determine the spatiotemporal evolution of the Lazufre volcanic area located in the central Andes, we combined short-term ground displacement acquired by InSAR with long-term geological observations. Ground displacement was first detected using InSAR in 1997. By 2008, this displacement affected 1800 km² of the surface, an area comparable in size to the deformation observed at caldera systems. The original displacement was followed in 2000 by a second, small-scale, neighbouring deformation located on the Lastarria volcano. We performed a detailed analysis of the volcanic structures at Lazufre and found relationships with the volcano deformations observed with InSAR. We infer that these observations are both likely to be the surface expression of a long-lived magmatic system evolving at depth. It is not yet clear whether Lazufre may trigger larger unrest or volcanic eruptions; however, the second deformation detected at Lastarria and the clear increase of the large-scale deformation rate make this an area of particular interest for closer continuous monitoring.

Zusammenfassung

Vulkanische Deformationen in großem Maßstab, die mittels InSAR gemessen wurden, liefern neue Informationen und dadurch einen neuen Blickwinkel auf vulkan-tektonische Aktivitäten und das Verständnis von langlebigen, magmatischen Systemen. Die Destabilisierung eines solchen Systems in der Tiefe beeinflusst dauerhaft die Oberfläche durch Versatz des Bodens, magmatische Einflüsse und vulkanische Unruhen.

Mit der Kombination aus kleinräumigem Bodenversatz gemessen mittels InSAR, numerischer Modellierung und langfristigen geologischen Beobachtungen, analysieren wir die Gegend um den Vulkan Lazufre in den Zentralanden, um die raumzeitliche Entwicklung der Region zu bestimmen. Bodenversatz wurde hierbei im Jahr 1997 mittels Radar-Interferrometrie (InSAR) gemessen, was eine Fläche von 1800 km² ausmacht, vergleichbar mit der Größe der Deformation des Kraters. Im Jahr 2000 wurde zusätzlich eine kleinräumige Deformation am Nachbarvulkan Lastarria entdeckt.

Wir sehen räumliche als auch zeitliche Verbindungen zwischen der Deformation des Vulkans und vulkanischen Strukturen innerhalb der betroffenen Gegend. Wir folgern daraus, dass diese Beobachtungen der Ausdruck eines langlebigen, magmatischen Systems in der Tiefe an der Oberfläche sind. Es ist noch nicht klar, ob Lazufre größere vulkanische Unruhen, wie zum Beispiel Eruptionen auslösen könnte, aber die Deformation am Vulkan Lastarria und ein Anstieg der großräumigen Deformationsrate, machen diese Region interessant für eine zukünftige, kontinuierliche Überwachung.

Chapter 1

Introduction

1.1 Goals and motivation

The main goal of this study is to improve our understanding of large magmatic systems using an approach that combines ground deformation (InSAR), numerical modelling and geological observations. The results presented here have several implications. Lazufre is a rare case of large-scale volcano deformation, with similar dimensions only observed elsewhere in caldera systems. Our results represent a new comprehensive analysis of large-scale volcanic complexes from remote sensing down to localised observations. Lazufre hosts two contemporaneous volcano deformations of different scales and different source depth locations. It is known that neighbouring volcanoes may interact, but the mechanisms at work are still not well understood. Using numerical modelling, we analyse the stress field induced by the inflation of a deep source and propose that changes in the induced stress field may have in turn triggered the reactivation of the second, shallow volcanic system. In addition, although these geodynamic processes affect and shape the volcanic arc, our results, based on volcanic unrest expressed in short-term surface deformations (InSAR) and long-term volcano lineament settings, may conversely provide information about regional tectonic activity through time.

1.2 Volcano-tectonic relationship

The intraplate stress regime in active tectonic areas influences the orientation of magmatic reservoirs and dikes (Nakamura, 1977a, Tibaldi, 1995). A subtle equilibrium between the regional stress field and the stress induced by the magma accumulation, as well as pre-existing structures and local gravitational effects, governs the structure and the shape of volcanoes (Fiske and Jackson, 1972; Takada, 1994; Acocella, 2003).

In this work, we combine classic structural mapping of volcano lineaments with the analysis of volcano deformation using InSAR with the aim of understanding the relationship between volcanic and tectonic activity. Lazufre hosts several volcano deformations that affect around 100 volcanic centres. Using InSAR, we observe at Lazufre a 1800 km² elliptical deformation that has its major axis oriented in the NNE-SSW direction. To place this deformation in its geological context, we perform a detailed analysis of the volcanic structures using remotely-sensed optical images and aerial photographs. We find a close relationship between the actual elliptical deformation, the volcanic vent concentrations and the orientation of vent lineaments. Both the deformation and the volcanic structures appear to be related in time and space and to be influenced by a constant remote stress field present since the Pleistocene (see details in chapter 4).

1.3 Large-scale volcano deformation

Recent large-scale surface deformation detected by radar satellite techniques (InSAR) in the volcanic area shows ground displacement affecting areas larger than 1000 km², as observed in Hualca Hualca, Uturuncu, Cerro Blanco and Lazufre in South America (Pritchard, 2002), at the Yellowstone and Long Valley calderas in North America (Chang et al., 2007; Tizzani et al., 2008) and at Uzon in Kamchatka (Lundgren and Lu.,

2006). These deformations are mostly related to caldera systems responsible in the past for large ash-flow eruptions with volumes up to 1000 km³ (Lipman, 1997; de Silva and Francis, 1991). In South America, however, these surface deformations are not directly related to clear caldera structures, with the exception of Cerro Blanco (Pritchard and Simons, 2002). The mechanisms responsible for these widespread ground displacements are not yet fully understood. Although the new input of deeper magma in a magmatic reservoir may induce transient observable surface deformation (Annen, 2009), hydrothermal activity alone may also produce large-scale ground displacement, as is observed at Yellowstone (Hurwitz et al., 2007) and Campi Flegrei (Gottsmann et al., 2003). Therefore, geodetic analysis alone provides only a partial understanding of the phenomenon and needs to be complemented with other approaches. While volcanic systems such as the Yellowstone, Long Valley and Campi Flegrei calderas are generally well monitored by complementary geophysical and geodetic studies, the Lazufre area was poorly studied before ground displacement was detected there in 1997 (Pritchard and Simons, 2002). The present study aims to implement InSAR data with complementary approaches to better understand the spatiotemporal evolution and activity change at Lazufre.

1.4 Methods used

1.4.1 Remote sensing observations

Remote sensing is the keystone of this study and provides observation data for both ground deformation analysis and structural analysis. These data are employed further in numerical modelling to understand the processes at work. For more than a decade, Interferometric Synthetic Aperture Radar technique (InSAR) has provided dense spatial maps of ground deformation that allow for the analysis of a deformation as an entity.

InSAR is a powerful tool that can improve our understanding of ground deformation and related mechanisms in volcanic areas. InSAR techniques use the phase difference (interferogram) between SAR image pairs separated in time, allowing one to obtain temporal and spatial surface displacement projected in the satellite line-of sight (LOS). Deformation time series may then be produced to obtain mean deformation velocity maps and time series with average standard deviation of 0.2 cm and ± 0.5 cm/yr, respectively (Casu et al., 2006).

To assess the tectonic context at Lazufre, we first map out volcanic features as eruptive fissures, as well as plotting vent locations and orientations. For this purpose, we use Landsat images with a ground resolution of 15 m after sharpening. Next, we georeference aerial photographs that partially cover the Lazufre volcanic area and surroundings.

These geodetic datasets are then inputted into a GIS platform that allows us to combine different results in a layered interface. For instance, Landsat and aerial photographs overlaid on a 30 m DEM facilitate classification of volcano typologies and also provide relative dating of the observed volcanic products, as well as permitting the determination of precise volcano orientations and related structures. This approach enables us to test potential relationships between InSAR deformation and mapped volcano features and to better understand recent large deformation in its volcano-tectonic context.

1.4.2 Field observations at Lazufre

In 2007 and 2008, field missions were organized at Lazufre and at the Lastarria volcano to install GPS and gravity benchmarks across Lastarria (Ruch, Le Corvec, Labazuy, Froger and Bonvalot) and a seismic network in and around the Lazufre volcanic area (PI Walter). These networks aim to provide a longer term perspective on the volcanic processes in action, complementing the InSAR observations with ground-truth analysis.

In the shorter term, these missions also shaped our understanding of Lazufre itself. GPS and gravity network results are not part of the present study, although future fieldwork at these sites will provide valuable information regarding changes in the deformation and better constrain the evolution of the source at depth.

In January 2008, GFZ (Walter, Luhr, Gunther, Ruch), Hamburg University (Dahm) and University of Chile (Legrand) organised a field mission to install a network of 23 broadband seismic stations covering the Lazufre area for a period of three months. These stations were intended to observe seismic activity possibly triggered by inflation of the deep magmatic source. Preliminary results show a low concentration of deep seismicity, with higher local seismicity close to the Lastarria volcano. From 1 to 18 March 2008, Ruch, Aguilera, Manconi and Chilean students set up a multi-parameter station in a fumarolic field (5200 m asl) located on the western flank of Lastarria during a test period of four days to assess possible variations in hydrothermal activity. A Lacoste-Romberg gravimeter sampled continuously at 1 Hz along with a pressure sensor and three thermocouples registering at high temperature fumaroles and at the gravimeter location. Although the results show very low gravity amplitude signal variations at the level of instrumental errors, we did register a remote earthquake and possible daily temperature variations.

In parallel, we developed a collaborative network with Chilean and French partners during this fieldwork that is of importance for future projects in the Andes:

- University Blaise-Pascal (France): Dr. J.-L. Froger and P. Labazuy
- IRD (France): Dr. S. Bonvalot
- Universidad Catolica del Norte (Antofagasta, Chile): Prof. E. Medina
- Universidad de Calama (Chile): Dr. F. Aguilera

- University of Chile (now at Mexico State University): Dr. D. Legrand

1.4.3 Modeling surface deformation

Surface deformation observed by geodetic techniques (InSAR, GPS, levelling, tiltmeter, gravity) may be an indirect indicator of magmatic and/or hydrothermal subsurface activity and/or mass movements. To obtain complementary information about the source at depth, analytical solutions based on simple geometry source models are also implemented in numerical models to analyse and assess the source characteristics (Mogi, 1957; Okada, 1985 & McTigue, 1985). We are thus able to retrieve information about the source location and evolution, estimating, for instance, its depth, volume and pressure change. Our models are run in a homogeneous elastic half-space domain. Although no additional geophysical or geological data are available at Lazufre at present to construct more realistic models, our findings provide first order information about the source characteristics. Future results from seismic tomography and GPS analysis will certainly improve our understanding of the source located below the Lazufre volcanic area.

1.5 Thesis organisation

The analysis and results presented in this manuscript represent a stepwise approach that addresses different aspects of volcano deformation with the overarching aim of gaining a clearer understanding of the Lazufre volcanic system as a whole. This project encompasses a detailed study of the geological structures present up to a general analysis of the deformation signal.

1.5.1 Caldera-scale inflation of the Lazufre volcanic area, South America: evidence from InSAR

In chapter 2, we used classic InSAR observations and numerical modelling to analyse the source characteristics responsible for the long wavelength signal, estimating depth, volume change and surface displacement for the period spanning 2003 to 2006 (**Ruch et al., 2008, published in JVGR**). We observed an increase of the uplift rate, which we attribute to a source expanding at 10 km depth. We argue that the deformation may be related to a long-lived magmatic system expanding at depth.

Author contributions: Anderssohn processed the interferograms, Motagh provided the inversion script. Ruch and Walter carried out the project. The analysis of the dataset, the geological study and the written manuscript were the work of Ruch under the supervision of Walter.

1.5.2 Stress transfer in the Lazufre volcanic area, central Andes

Although we discuss and analyse the long-wavelength signal of the Lazufre deformation in chapter 2, Froger et al. (2007) detected a second local deformation affecting the Lastarria volcano. In chapter 3, we test a possible relationship between both systems, explaining them with a deep source for Lazufre and a shallow source for Lastarria. Using InSAR time series (Berardino et al., 2003) spanning 1996 to 2008, we observed a possible time delay separating the deformations. Using a numerical model, we propose in the second chapter (**Ruch et al. 2009, published in GRL**) that a deep inflating reservoir increased the tensile stress close to the surface, thus possibly triggering the deformation observed at Lastarria.

Contributions: IREA colleagues (Zeni, Solaro, Peppe, Lanari) processed the InSAR time series datasets, Shirzaei provided an inversion code for Lastarria, Walter, Manconi and

Ruch carried out the project, Ruch analysed the dataset with the collaboration of Manconi and Ruch wrote the manuscript under the supervision of Walter.

1.5.3 Short-term and long-term volcano deformations as potential stress field indicator in the central Andes

Although geodetic observations alone provide limited information about the long-term (10^{2-3} years) evolution of Lazufre, in chapter 4, we analyse the volcanic features located inside and in proximity to the deforming area (***Ruch & Walter. 2010, published in Tectonophysics***). We used remote sensing data (Landsat, aerial photograph) to assess the volcanic structures and found that the deforming area (InSAR) contains a higher concentration of volcanic vents than the surroundings. We further propose that both short-term (InSAR) and long-term (volcano lineaments) observations may be used as complementary proxies to assess the stress field orientation in the volcanic arc since the Pleistocene.

Contributions: Strecker and Walter shared fruitful discussions with Ruch during the concept development; Lanari provided the InSAR dataset. The author undertook both the remote sensing analysis and the writing under the supervision of Walter.

1.5.4 Salt lake growth detected from space

Beside volcano deformation, the surroundings of the Lazufre area host several other local, non-volcanic deformation types as observed at salars and on volcano flanks (see chapter 3). Chapter 5 is an example of how full InSAR datasets may be analysed to better assess the deformation mechanisms. Using high-resolution InSAR data combined with ground truth geochemical data and ground composition obtained from Landsat images, we propose that the deformation is the result of salt precipitation and accumulation, driven by capillarity and crystallization process. These results were

presented at an International Congress and will be submitted soon in a peer-reviewed journal.

Contributions: Risacher and Warren provided expertise regarding the physical and chemical properties of evaporates, and Lanari provided the InSAR dataset. Ruch elaborated on the concept with the collaboration of all authors, while the analysis of the dataset and the writing was done by the author.

Chapter 2

Caldera-scale inflation of the Lazufre volcanic area, South America: evidence from InSAR

J. Ruch, J. Anderssohn, T.R. Walter, M. Motagh

GeoForschungsZentrum Potsdam, Telegrafenberg, D-14473, Potsdam, Germany

Abstract

Collapsed calderas are the structural surface expression of the largest volcanic eruptions on Earth and may reach diameters of tens of kilometres while erupting volumes larger than 1000 km^3 . Remnants of collapse calderas can be found along the South American volcanic arc and are thought to be inactive. However, this study shows that systems of such dimension may become active in a relatively short period of time without attracting much attention. Using satellite-based InSAR data, a 45 km wide elongated area of ground deformation was observed in the Lazufre volcanic region (Chile), where no deformation was detected 10 years ago. The deformation signal shows an uplift of up to $\sim 3 \text{ cm yr}^{-1}$ during 2003-2006, affecting an area of about 1100 km^2 , comparable in size to super-volcanoes such as Yellowstone or Long Valley. This deformation signal can be

explained by an inflating magma body at about 10 km depth, expanding and propagating laterally at a velocity of up to 4 kilometres per year. Although it is not clear whether this intrusion will lead to an eruption, its dimensions and the rapid deformation rate insinuate that a potentially large volcanic system is forming.

2.1 Introduction

Collapse calderas are subcircular depressions in volcanic areas that are thought to form during rapid evacuation of a shallow crustal magma chamber and are associated with the most devastating type of volcanic eruptions (Lipman, 1997; Williams, 1941). No major caldera-forming eruptions have been witnessed by mankind, except for the Minoan eruption on the Santorini Island (~3600 BP) and the Great Toba caldera eruption (Indonesia) at 71,000 BP that is thought to have drastically reduced the genetic diversity of the human population (Ambrose, 1998). Although the processes acting during caldera eruptions have been extensively studied in the field and laboratory (Cole et al., 2005), the early development of magmatic systems responsible for such eruptions remain poorly understood and controversial. It is well accepted in the literature that large calderas are associated with large crustal magma chambers (Cole et al., 2005; de Silva, 1989; Francis et al., 1989; Ort et al., 1996; Lipman, 1997). However, such magma bodies at depth are seldom geophysically constrained and clear evidence of *in situ* magma reservoirs beneath volcanoes is rare (Marsh, 2000).

The subduction of the Nazca plate beneath South America is responsible for the uplift of the Altiplano-Puna plateau (16°S-26°S), part of the Central Volcanic Zone (CVZ, 14°-28°S). The thickening of this high - elevated zone leads to extensive crustal melting (de Silva, 1989) that has resulted, during the last 20 million years, in one of the most voluminous explosive volcanic provinces in the world. Caldera collapses and associated

ignimbrite deposits represent the dominant type of volcanism in this area, partially superimposed by younger stratovolcano edifices. Chile hosts 36 historically active volcanoes and 16 major calderas, with diameters of up to 50 km (Lipman, 2000). The Altiplano-Puna plateau is known for its abundance of ancient large caldera collapses that occurred in geologic times, examples being La Pacana (60x30 km, long and short axis diameters, respectively), and Cerro Galán (35x20 km).

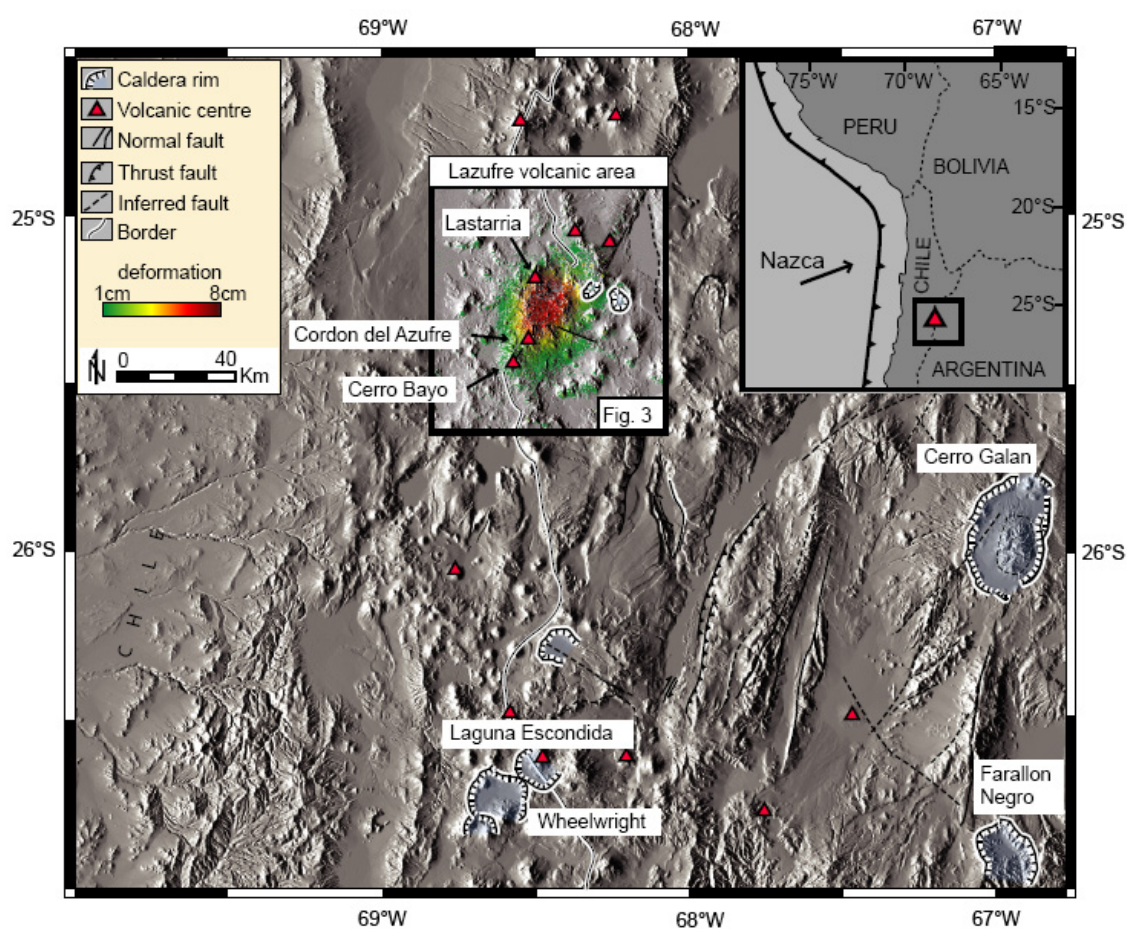


Figure 1: Shaded relief map of the central Chile volcanic arc and the location of the inflation at the Lazufre volcanic area. Older caldera systems are shaded in light blue, with faults are marked by black lines.

In this work we focus on the Lastarria-Cordon del Azufre volcanic area (“Lazufre” after Pritchard and Simons, 2002), a region composed of about 40 Quaternary volcanic centres surrounded by older caldera systems (Figure 1). Inflation of up to $\sim 1 \text{ cm yr}^{-1}$ during the period 1996-2000 was first observed using satellite SAR interferometry

measurements by Pritchard and Simons (2002, 2004). A more recent study showed that the rate of inflation had increased, such that at around 2005 it was 2.5 cm yr^{-1} (Froger, 2007). Here we analyse newly acquired SAR data from the Envisat satellite for the period 2003 to 2006 to better assess the temporal and spatial evolution of surface deformation at Lazufre, and to determine its source parameters. Analysis of the data suggests that the extent and rate of inflation is further increasing. Using a time series analysis, we are able to constrain the volume change and discuss the dimension of a proposed magma reservoir underlying this area.

2.2 The 2003 – 2006 deformation

2.2.1 InSAR data

In order to study land-surface deformation in the Lazufre area, we selected 11 Envisat SAR images acquired in descending orbit covering the period between

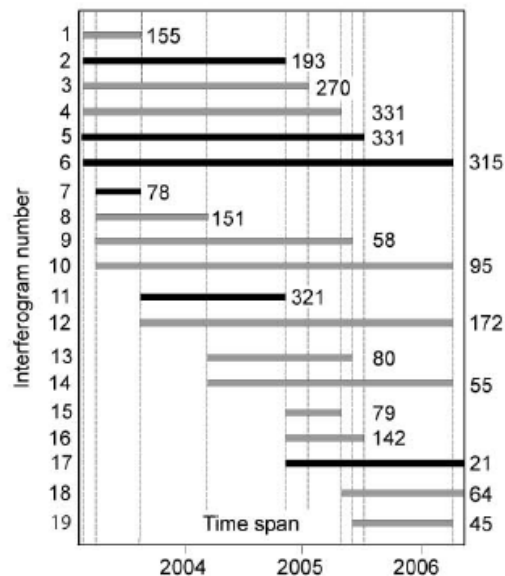


Figure 2: Time series of the 19 radar interferograms showing deformation at Lazufre from March 2003 to June 2006. The interferograms used for the deformation rate calculations are shown by bold black lines. The numbers on the left are the interferogram's numbers used in the text. The numbers on the right denote the perpendicular baseline in meters.

March 2003 and June 2006. We processed the data using the software package SARscape (www.sarmap.ch) and generated 19 interferograms with perpendicular baselines ranging between 20 and 330 m (Figure 2). A 3 arc-second SRTM digital

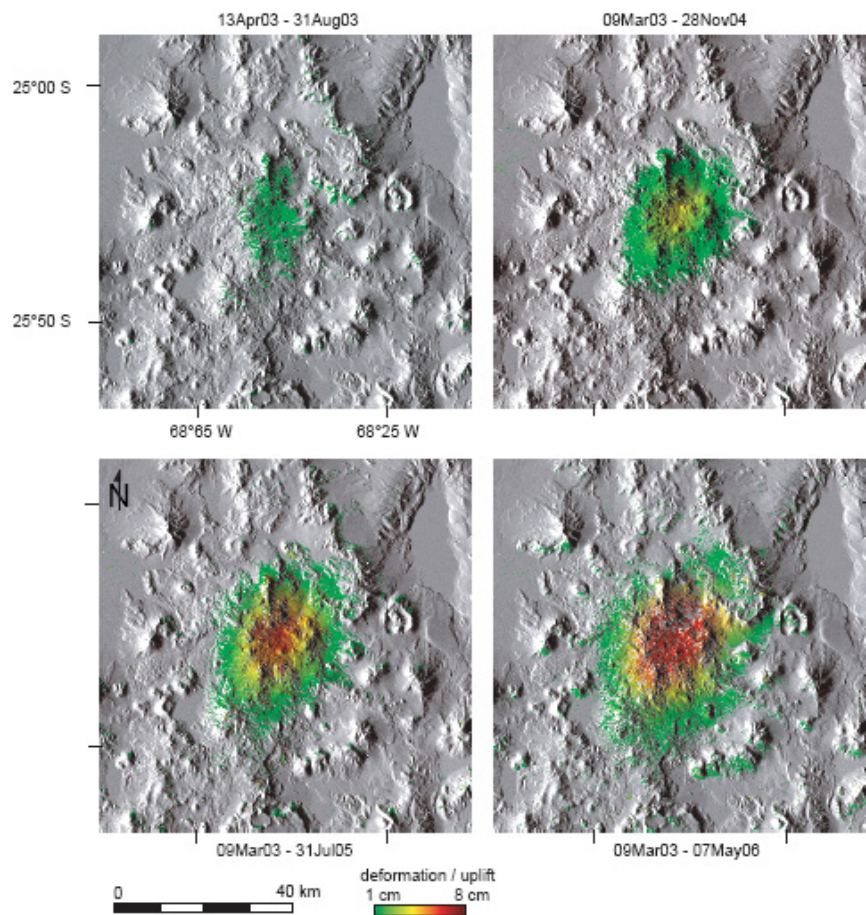


Figure 3: Unwrapped InSAR data for different temporal baselines. Note that the area and amount of uplift increases with time and that the area of the deformation contains several volcanic centres.

elevation model was used to correct for topographic effects and to geocode the interferograms. The differential interferograms were unwrapped using a growing region algorithm (Reigber and Moreira, 1997) to determine the absolute value of the range change. To reduce the InSAR typical noise we applied a low - pass Kernel filter on the geocoded unwrapped results and applied pair-wise logic to discriminate between the displacement signal and atmospheric artefacts (Massonnet and Feigl, 1998).

Interferograms that show significant artefacts due to topographic, atmospheric or orbital errors were not considered in this study. However, the accuracy of InSAR measurements is still difficult to quantify due to the complexity of the cumulative error estimations (Bürgmann et al., 2000 Massonnet & Feigl 1998). The coherence of the InSAR pairs in the region is generally high for the observation time period of interest that is between 2003 and 2006. Figure 3 shows four examples of the interferograms covering time intervals of 0.5 to 3.2 years. The interferograms show the LOS (line-of-sight) displacement, where both the amount and spatial extent of the signal appear to increase with time. The maximum displacement rate is hence $2.8\text{-}3\text{ cm yr}^{-1}$ for the observation period 2003-2006, which is ~ 3 times more than that deduced from earlier InSAR observations for the period 1998-2000 (Pritchard and Simons, 2002) and slightly more than that estimated for the period 2003-2005 (Froger et al., 2007).

2.2.2 Volume and area increase

We now investigate the increasing rate of surface deformation by analysing the volume evolution of the uplifted area. We use interferograms with time spans from 140 up to 1155 days to compute incremental volume changes with time. We mask out the dataset below one centimetre to avoid the integration of sparse signals present below this threshold. For comparison we select four interferograms that start in 2003 (similar master image) with different time intervals (dissimilar slave images). These volumes are normalized with respect to the time interval they span to obtain the mean annual uplift rate. The results are shown in Figure 4a. Over the considered time interval, the mean rate of inflation increased from about 3 ± 1.5 to $6 \pm 0.74 \times 10^6\text{ m}^3\text{ yr}^{-1}$. The area affected by the deformation enlarged from about $300 \pm 158\text{ km}^2\text{ yr}^{-1}$ to $900 \pm 124\text{ km}^2\text{ yr}^{-1}$ (Figure

4b). We tested this rate by selecting another set of InSAR data, where the

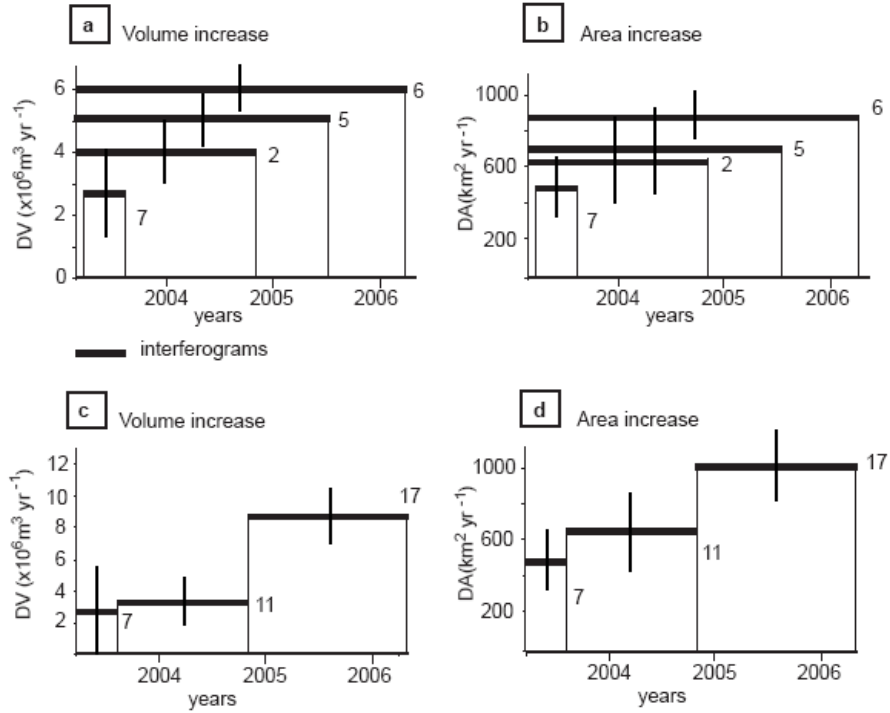


Figure 4: Time series plots showing the increase of the volume and the area of the surface displacement at Lazufre. Four normalized unwrapped interferograms span the period 2003-2006. Interferograms n° 2, 5 and 6 have the same master image, while interferogram n° 7 has a master image that is close in time (35 days) to the former. The same trend is observed using three other normalized independent interferograms (c, d). Vertical bars indicate the standard deviation assuming 1 cm deviation in the InSAR measurements.

slave image of the first is the master image of the second interferogram, and so on. These yielded volume increases from 3 ± 1.5 to $9 \pm 1.9 \times 10^6 \text{ m}^3 \text{ yr}^{-1}$, and area increases from $300 \pm 158 \text{ km}^2 \text{ yr}^{-1}$ to $1000 \pm 320 \text{ km}^2 \text{ yr}^{-1}$ (Figure 4c, d). The rates of increase are thus very similar in both cases. As we will show in the next section, the deformation source underlying the Lazufre area is therefore increasing in its dimensions.

2.2.3 Source modelling

In order to characterise the source of the inflation, we performed an inversion in a two-step process. First, we constrain the depth of the source by applying a homogeneous

dislocation source, and second, we discretize this source into smaller elements and calculate the distribution of opening.

The InSAR data are fitted using Okada's formulation (1985) to estimate the length, width, depth and uniform opening of a dislocation plane. Regarding the shape of the surface displacement, we constrained the strike (direction of deformation), the ratio

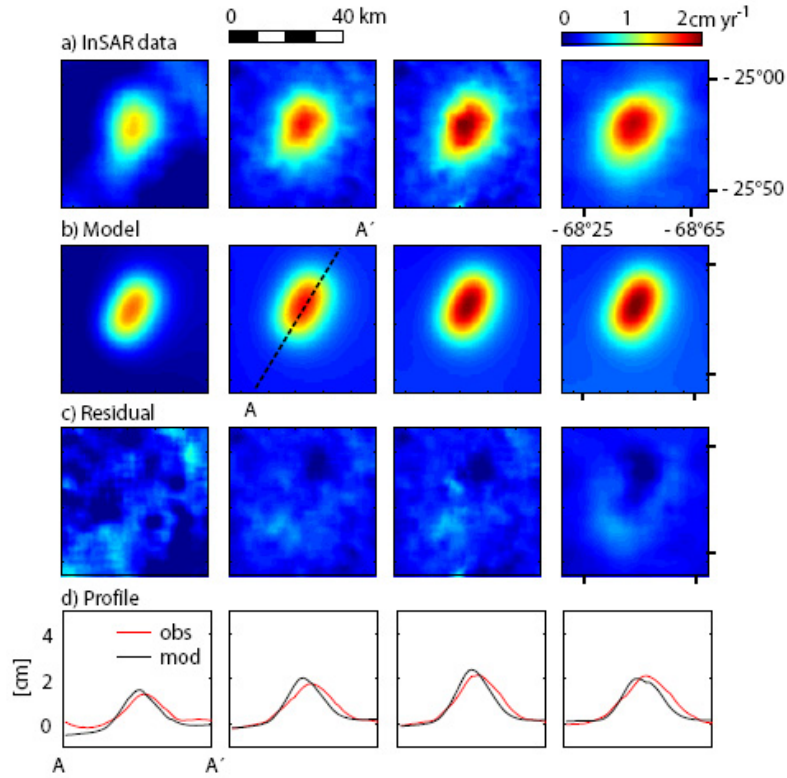


Figure 5: InSAR data inversion using Okada's formulation for the four studied interferograms: 1) 13Apr03-31Aug03, 2) 09Mar03-28Nov04, 3) 09Mar03-31Jul05, 4) 09Mar03-07May06. a) Normalized unwrapped InSAR data is showing uplift up to 3 cm yr^{-1} with increasing area. b) Model simulations with a horizontal rectangle dislocation source (Okada, 1985) located at 10 km depth. c) Residual test between the InSAR data and the models show a good fit.

between the length and the width, and define the source as horizontal. The inversion is done using a non-linear Levenberg-Marquardt algorithm via the minimization of the mean square misfit (Tarantola, 1987). We find that, for the interferograms inverted, sources with depth from 8.5 to 13 km provide reasonable fit to the data. Figure 5 shows

the normalized InSAR data, together with the best fitting models derived from the inversion.

In the second working step, we constrain the optimal depth to be at 10 km, enlarge the horizontal plane at lateral edges and discretize it into smaller triangular elements (see also Lundgren and Lu, 2006). We solve for opening on each of the elements

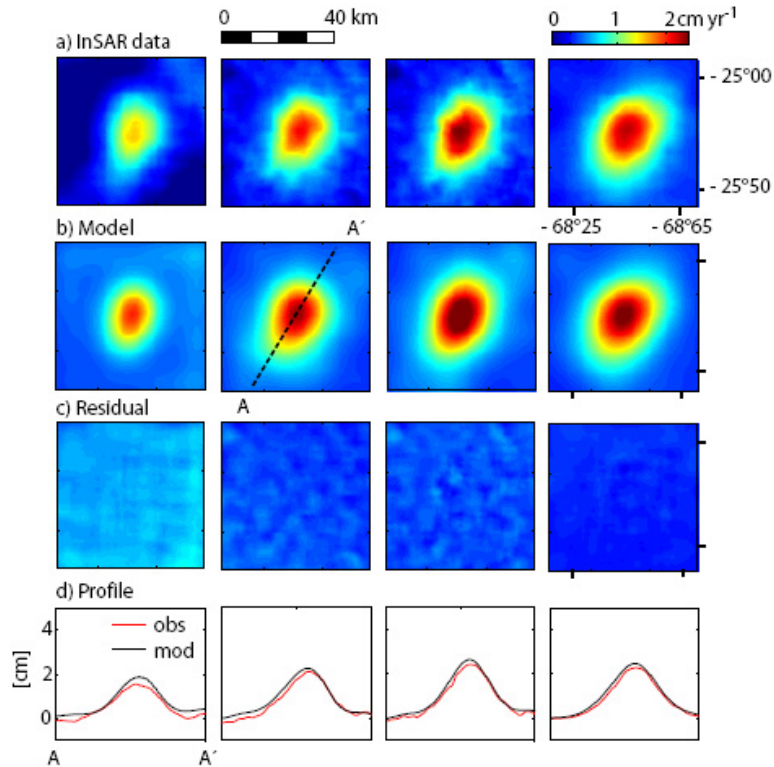


Figure 6: InSAR data inversion using distributed slip (observation data as in Figure 5) a) Normalized unwrapped InSAR data, b) Horizontal distributed slip model simulations c) Residual test between the InSAR data and the models.

using a linear inversion implemented by a boundary element approach (Maerten et al., 2005; Thomas, 1993). Compared to the homogeneous slip models, the distributed slip models show better fits to the InSAR data due to the geometry of the source (Figure 6). The slip distribution suggests a maximum opening of 5 to 6 cm yr^{-1} (Figure 7), equivalent to a fluid overpressure of about 20 MPa, assuming a mean value of 75 GPa for the crust rigidity. Moreover, by comparing the opening distributions for the various

interferograms, we obtain information about the lateral expansion of the source.

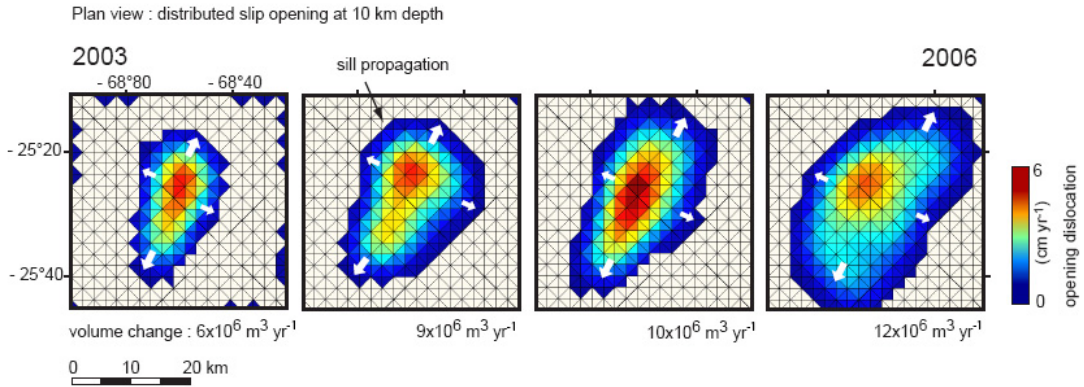


Figure 7: Dislocation plane models showing slip distribution at 10 km depth using normalized interferograms from 2003-2006. The peak of opening is about 6 cm yr^{-1} for all the dislocation models, whereas the source propagates laterally at a velocity of about $1\text{-}4 \text{ km yr}^{-1}$. These models are consistent with a laterally expanding magma intrusion.

As shown in Figure 7, the source laterally expands with time, while the rate of volume change doubles over the 3-year time-period, from $6 \times 10^6 \text{ m}^3 \text{ yr}^{-1}$ to $12 \times 10^6 \text{ m}^3 \text{ yr}^{-1}$. This is several orders larger than common rates in arc volcanoes (Ingebritsen et al., 1989). Our models suggest that the source expands from about 300 to 650 km^2 and is elongated in a NNE-SSW direction. An important implication is that the axes of the source propagate horizontally at a rate of up to about 4 km yr^{-1} , respectively. Although the total difference of volume (ΔV) of this assumed magma body is not yet comparable to that of ashflow systems, the spatial dimension of the source and the surface doming is already comparable to that of the largest known calderas. As discussed below, however, the total volume of the source may be much larger than its currently observed volume changes.

2.3 Discussion

During the Quaternary period, about 130 large calderas erupted worldwide (Newhall and Dzurisin, 1988). Of these, about 10 caldera volcanoes are currently in a state of unrest (Siebert and Simkin, 2002-) and only a few are closely monitored. One main difficulty is

to detect and characterise the magma storage system, an important variable for volcano hazard assessment. As caldera formation requires a shallow crustal magma chamber, the latter could be detected prior to caldera evolution. In this study, we use InSAR data to obtain insights into the evolution of a volcanic area subject to inflation that may be linked to a >30 km diameter magma chamber. Our InSAR data suggest that the extent of uplift > 1 cm is about 1100 km², centred at 25.25°S and 68.49°W. As proposed by Pritchard and Simons (2004), deformation in this region most probably started in early 1998 and may be related to magma intrusion. Our study reveals that this process continues and has even increased its rate of volume accumulation. We find that the detected normalized displacement rate tripled from 2003 to 2006, and the rate of volume increase has doubled over the same period.

2.3.1 Limitations of the models

Important informations for Lazufre volcano complex were retrieved from InSAR data, however, we note that data handling and model building may depend upon the a-priori information available for the study object and the methods applied. Implementations with additional geophysical and petrological data can reduce a part of the actual limitations. The lack of such information does not support more complex model simulations including, for example, crustal heterogeneities that are known to have important effect on the source parameters (Manconi et al. 2007). Uncertainty exists in the source location, strength and finite geometry. For instance, subvertical displacement data alone, without additional horizontal displacement measurements, is limited to constrain unambiguously the geometry of the deformation and subsequently the source parameters (Dieterich and Decker, 1975). Besides modelling limitations, errors in geodetic data may also significantly effect the interpretation. The accuracy of InSAR measurements is still difficult to quantify due to the complexity of the cumulative error

estimations (Bürgmann et al., 2000; Hanssen, 2001; Massonnet & Feigl 1998), and even under ideal conditions, only centimetre accuracy can be estimated in many cases. Therefore, our hypothesis and data interpretation may be influenced by the data quality, atmospheric and topographic artefacts, and filtering techniques applied, as well as simplifications that were necessary for the model calculations.

2.3.2 Multiple source evidence

Froger et al. (2007) proposed a second, smaller source of deformation in the northern part of the anomaly of Lazufre. This smaller source, located one kilometre beneath the Lastarria volcano, is interpreted to represent shallow hydrothermal activity. In this study, we performed a different modeling strategy and therefore obtain slightly different results. While Froger et al. (2007) used uniform source model geometries constrained by InSAR observations to fit the surface deformation pattern, we use distributed slip models. Both are valid methods and complementary approaches and both well reproduce the InSAR signal. Our approach does not resolve the second shallow source, however, it brings new insights into the evolution of the source at depth and allows the estimation of the spatio-temporal evolution and propagation of the intrusion.

2.3.3 The comparison to other inflation caldera systems

The InSAR data presented herein shows that the diameter of the surface inflation is 45x30 km wide. This dimension implies the presence of an extended magma body, which is also supported by geomorphology: The area displays a regional topographic dome of about 500 m height which has a central depression crowned by a ring of Quaternary volcanoes (Froger et al., 2007; Pritchard & Simons, 2002). In addition, three

major volcano lineaments represented by the Lastarria, two unnamed important

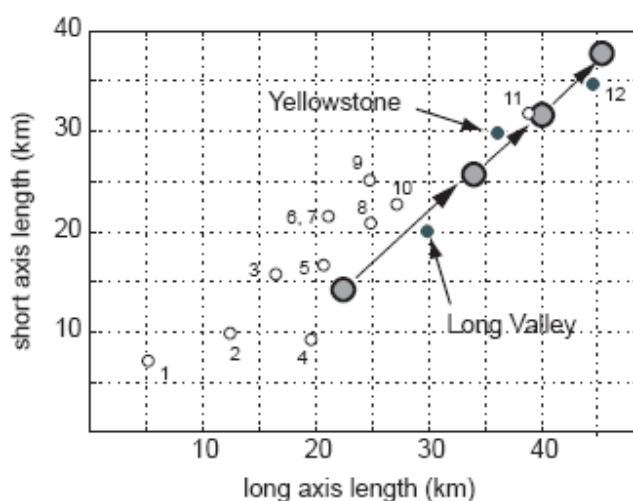


Figure 8: Ground deformation of volcanic area larger than 5 km in diameter, as measured by InSAR. The periods of observations are from 1996-2000 for Yellowstone (Wicks et al., 2006); 1997-1998 for Long Valley (Neumann et al., 2006), while the red dots show the evolution of Lazufre from 2003 to 2006. The other large systems are: 1) Sierra Negra (Galapagos islands), 2) Seguam island (Alaska), 3) Hengill volcano (Iceland), 4) Three Sisters (North USA), 5) Uzon caldera (Kamchatka), 6) Makushin (Alaska), 7) Cerro Blanco (Argentina), 8) Eyjafjallajökull (Iceland), 9) Mount Peulik (Alaska), 10) Westdahl (Alaska) and 11) Uturuncu (Argentina).

volcanic fissures, Cordon del Azufre and Cerro Bayo converge radially to the central depression (see Figure 1). A dome and an apical depression crowned by a ring of volcanic centres are typical features for regions of inflation and of pre-caldera collapse stages (see also Lipman, 2000).

In order to better place these dimensions in a global context, we compare different inflation regions detected by InSAR. Figure 8 is a compilation of selected recent works at volcanic areas subject to inflation larger than 5 km in diameter. We retrieve approximate diameters from previous geodetic studies (Amelung et al., 2000; Feigl et al., 2000; Lu et al., 2000, 2002a, 2002b, 2002c; Lundgren and Lu, 2006; Masterlark and Lu, 2004; Newman et al., 2006; Pedersen and Sigmundsson, 2004; Pritchard and Simons, 2002; Wicks et al., 2006) and add also the dimension of the Lazufre area for the four observed periods shown in Figure 3. Figure 8 shows, for instance, that only a few

other volcanic systems show deformations comparable in size, namely Yellowstone and Long Valley in the USA, Uzon caldera in Kamchatka and the Hualca Hualca volcanic area in Peru (Lundgren, 2006; Pritchard and Simons, 2002; Wicks et al., 2006). The Lazufre volcanic area has increased in size from about 300 km² to 1100 km², with an average diameter from ~ 20 km to ~ 45 km (Figure 8), suggesting that Lazufre has the potential to become the largest deforming volcano system on Earth.

2.3.4 Source origin

Recent studies of caldera systems have proposed that hydrothermal activity instead of magma may cause ground displacements (Battaglia et al., 2006; Gottsmann et al., 2003; Hurwitz et al., 2007). However, Lazufre shows no evidence for major hydrothermal activity that could be responsible for the observed deformation pattern, with hydrothermalism appearing to be limited to the fumarole activity on the Lastarria volcano (Froger et al., 2007). Moreover, we believe that due to the buoyancy of hydrothermal fluids, they may prefer a vertical propagation direction rather than the horizontal propagation as identified by our InSAR time series models. Nonetheless, ongoing ground-truth data, such as repeated microgravity campaigns and seismic studies, will help to better constrain the nature of the source.

We herein consider that the lateral expansion at depth is related to magma propagation, supposing an intrusion at the level of neutral buoyancy (Ryan, 1987). This depth is slightly deeper than that based on thermobarometry studies of the Neogene ignimbrite products in the CVZ (Central Volcanic Zone), that show evidence of mineral phases in equilibrium typically in the depth range of 5 to 9 km (Schilling et al., 2006). We note that the lower bound of our calculated source depth location is within this range, dependent upon the constraints applied during the inversion. Our magma intrusion hypothesis is in agreement with a study of the Puna plateau 200 km to the north, in

which other authors propose that sub-horizontal crustal faulting is associated with mid crustal-magma sheet intrusions (Riller and Oncken, 2003).

2.3.5 Earthquake triggering of magma intrusion

Of special interest is the question, why did the inflation of the Lazufre abruptly start in 1998. A connection with a series of tectonic-based earthquakes from 1995-1998 surrounding the Lazufre area may have encouraged a possible magma intrusion (Pritchard 2002). The megathrust M8.1 Antofagasta earthquake, which occurred in June 1995, was followed by a series of $M > 6$ earthquakes along with a M7.1 event in January 1998, located 250 km WNW from Lazufre. These events coincide with the start of the surface deformation observed at Lazufre. Earthquakes may have reactivated pre-existing structural weak zones in the volcanic arc and, hence, destabilized an existing magma body (Walter and Amelung, 2007). Alternatively, the passing seismic waves may also have triggered a perturbation of a magma reservoir (Manga and Brodsky, 2006).

2.3.6 Total volume of the source

Due to the absence of satellite data for the period 2000-2003, it is difficult to assess the total volume of the source since the start of deformation in 1998. ERS1/2 satellite data yield a volume-change rate of $6 \times 10^6 \text{ m}^3 \text{ yr}^{-1}$ from 1998 to 2000 (Pritchard and Simons, 2004), whereas our Envisat data show that rate increases from $6 \times 10^6 \text{ m}^3 \text{ yr}^{-1}$ to $12 \times 10^6 \text{ m}^3 \text{ yr}^{-1}$ from 2003 to 2006. Assuming that the rate of inflation for the period 2000 to 2003 was the same as for the period 1998-2003 and then increased from 2003 to 2006, a total volume of 0.05 km^3 may have been accumulated. This result is only representative of the difference in volume (ΔV) after a perturbation of the source. We emphasize that this does not necessary suggest a thin sill intrusion. We hypothesize that the source of the

deformation could alternatively be related to the inflation of a larger, pre-existing

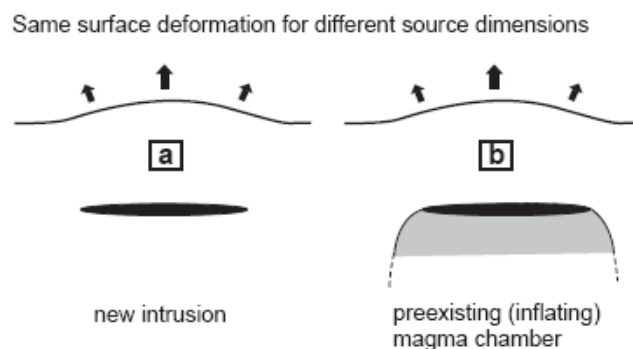


Figure 9: Two scenarios that may equally well explain the pattern of the source geometry of the surface deformation at Lazufre. a) A sill expanding laterally at depth, and b) a larger, pre-existing magma chamber inflating at depth.

magma body previously in a state of equilibrium (Figure 9). Earlier studies at a Galapagos caldera illustrated that a large magma chamber with a flat roof can produce the same amount and pattern of surface displacement as a thin sill (Yun et al., 2006). The finite source of the deformation at Lazufre may therefore be much larger than the volume change estimation presented here.

Evaluation of the thermal cooling of a magma body in a host rock may provide further insights on the dimension of the magma body (using standard thermal cooling estimates and ignoring the latent heat, see equations 4-149 - 4-150 in Turcotte and Schubert, 2002). Our InSAR data can be explained by a sill intruding at a rate of 6 cm yr^{-1} with a length of 35 km. If we consider a difference of temperature of 1000 K between the host rock and a sheet-like intrusion, the latter will completely solidify in about 1.5 hours. InSAR data, however, shows a constant inflation over a time series of 9 years, implying that the magma body must be larger in order to remain fluid. We now follow an approach applied by Yun et al., (2006) and inversely calculate the minimum magma chamber thickness required for 9 years long intrusion duration. Assuming that the source

of the Lazufre deformation has been constantly active since 1998 – 2006, the initial thickness of the magma chamber would have been at least 30 m (for a 1000 K temperature difference). Based on this result, the volume of the source would have been at least 6 km³. These models are very simplified, but provide a first order estimation of a much larger and yet realistic magma body volume.

2.4 Conclusion

InSAR data reveal a wide, elliptical ground inflation area with a long axis ~ 45 km in length and a LOS displacement of up to 3 cm yr⁻¹. The volume and area involved suggest a continuously-increasing rate since 2003. We interpret the source of the inflation as a magma body up to 30 km in diameter, located at about 10 km depth. Even though it is unclear if this rapid and wide deformation is a precursor of an eruption at Lazufre, this study implies that apparently inactive zones may become subject to deformation and develop into large dimension systems within a matter of a few years. The total volume of the entire magma body remains unclear. The InSAR data shows a volume change of 0.05 km³, which probably reflects only a minor part of a larger magma reservoir.

2.5 Acknowledgements

We are grateful to Paul Lundgren and an anonymous reviewer for their constructive comments which helped us to improve the manuscript and we appreciate discussions with Andrea Manconi. Envisat data were provided by the European Space Agency as part of category 1 project # 3455. The Research has been partially funded by the Deutsche Forschungsgemeinschaft (Emmy Noether grant, DFG #WA1642 and #MO1851/1-1), and the Geotechnologien programme 265.

Chapter 3

Stress transfer in the Lazufre volcanic area, central Andes

J. Ruch^{1,2}, A. Manconi^{1,3}, G. Zeni³, G.Solaro^{3,4}, A.Pepe³, M.Shirzaei¹, T.R.Walter¹,
R.Lanari³

¹Deutsches GeoForschungsZentrum (GFZ), Potsdam, Germany

²Dipartimento di Scienze Geologiche Roma Tre, Roma, Italy

³IREA-CNR, Napoli, Italy

⁴INGV-Osservatorio Vesuviano, Napoli, Italy

Abstract

In the present paper we generated a 13-year InSAR time series from 1995-2008 to investigate the spatiotemporal characteristics of two neighboring volcano's deformations for the Lazufre volcanic area, central Andes. The data reveal two scales of uplift initiating during the observation time: (1) a large-scale uplift started in 1997 that shows an increase of the mean uplift rate of up to 3.2 cm/yr, now affecting several eruption centers situated in an area larger than 1800 km² and (2) a small-scale uplift located at Lastarria volcano, which is the only volcano to show strong fumarolic activity in decades, with most of the clear deformation not observed before 2000. Both the large and small inflation signals can be explained by pressurized magmatic or hydrothermal

sources located at about 13 km and 1 km deep, respectively. To test a possible relationship, we use numerical modeling and estimate that the deep inflating source increased the tensile stress close to the shallow source during the period preceding the first sign of deformation observed at Lastarria. We discuss how the deep inflating source may have disturbed the shallow one and triggered the observed deformation at Lastarria.

3.1 Introduction

Stress field changes in volcanic areas have often been hypothesized to be responsible for sudden, unexpected eruptions at volcanoes that are close to a critical state (Hill et al., 2002). However, the importance of stress changes associated with adjacent volcanoes is poorly documented, and responsible processes are not well understood. Here we investigate two overlapping deformation signals affecting the Lazufre volcanic area and the Lastarria volcano, and stress field change model suggest a possible relationship.

The Lazufre volcanic area (central Andes) is located on the Chilean-Argentinean border about 300 km east of the subduction trench (Figure 1a). It is part of the highly elevated Altiplano Puna Plateau that started to form during the Eocene period, resulting from the convergence of the Nazca and the South American plates (Oncken et al., 2006, and references therein). The area contains several morphologically distinct volcanic centers (De Silva & Francis, 1991). Only one of these, the Lastarria volcano (~ 5700m asl), shows strong and persistent fumarolic activity localized on the recent crater borders and on the western flank (Figure 1f). No historic eruptions have been reported (Naranjo & Francis, 1987).

Through InSAR (interferometric synthetic aperture radar) studies, a large-scale elliptical deformation signal was detected during the period from 1998 to 2000 with a deformation rate of about 1cm/yr (Pritchard & Simons, 2002). At that time, the inflation

dimension reached about 35 km across the long axis (Pritchard & Simons, 2004),

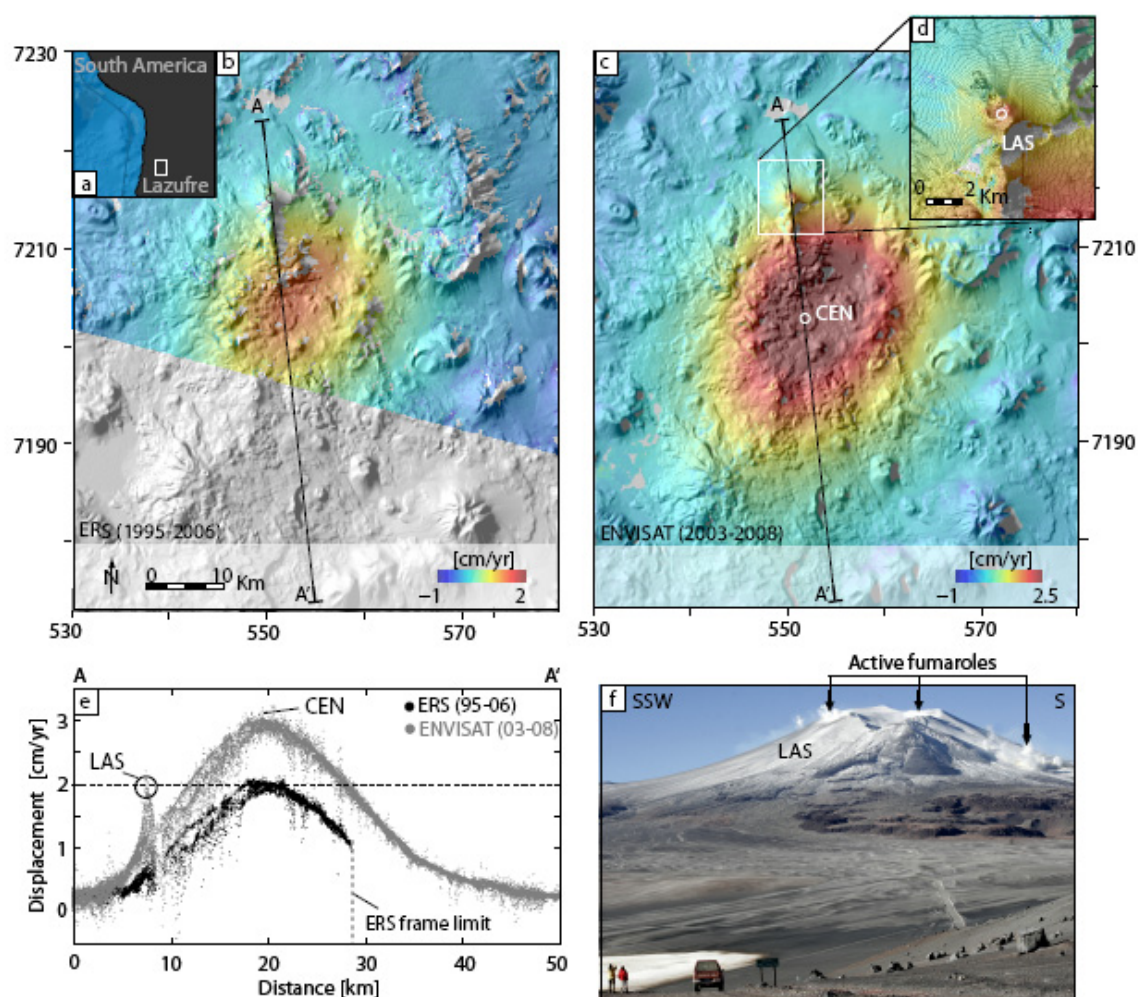


Figure 1: Deformation at the Lazufre volcanic area in the Central Andes. a) Location of Lazufre. Shaded relief maps with InSAR observation for b) the period from June 1995 to December 2006 (ERS) and c) the period from April 2003 to January 2008 (ENVISAT). d) Details of Lastarria volcano. e) NNW - SSE profiles across the deformation areas for the ERS dataset from 1995 to 2006 (black) and for the ENVISAT dataset (grey) from 2003 to 2008. Sampling width of the cross section is 1km. f) Photograph of the Lastarria volcano taken the 27th of April 2007 (9 a.m.) from the northwest (10 km distant from the summit).

and then increased up to 50 km (Froger et al., 2007, Ruch et al., 2008). Source depth estimates are between 9 and 17 km, probably related to magma intrusion (Pritchard & Simons, 2004). In addition, a second inflation signal, occurring at a smaller scale and affecting the Lastarria volcano was revealed. A very shallow pressurized source located

at ~ 1 km beneath the surface was used to explain the Lastarria deformation for the period from 2003 to 2005 (Froger et al., 2007). Nevertheless, the timing of these inflating volcanic systems as well as their relationship have not yet been evaluated.

Here we investigate the temporal relationship between the two revealed deformation signals by carrying out an advanced analysis on InSAR data spanning from 1995 to 2008. In addition, through numerical modeling, we suggest that the stress changes caused by the inflation of the deep source probably triggered the activity observed at Lastarria by increasing the tensile stress in the surroundings of the shallow source.

3.2 Deformation measurements

Two SAR datasets acquired by the European Satellite missions ERS-1/2 and ENVISAT, operating in descending orbits were used in this study (track 282, frame 4118). The ERS dataset includes 21 images spanning the period from June 1995 to December 2006, while the 24 ENVISAT acquisitions span from March 2003 to January 2008. Both datasets are relevant to the same illumination geometry ($\sim 23^\circ$ look angle). The phase difference (interferogram) between temporally separated SAR image pairs has been exploited via InSAR techniques (Massonet & Feigl, 1998) to get an estimate of the ground deformation projection in the radar sensor's line-of-sight (LOS). We computed a total of 153 interferograms characterized by spatial baseline values smaller than 500 m. To retrieve the mean deformation velocity maps of the area and the corresponding displacement time series, we applied the SBAS algorithm (Berardino et al., 2002), which also allows the filtering of possible atmospheric artifacts (see 3.7 Auxiliary materials). Because spatially the ERS and the ENVISAT acquisitions only partially overlap (Figure 1b-c), the SBAS analysis has been performed separately on the two datasets. Accordingly, we obtain two mean deformation velocity maps and 13-year displacement

time series within the overlapping region with a standard deviations of about 0.1 - 0.2 cm/yr and 0.5 - 1 cm, respectively (Casu et al., 2006).

The retrieved deformation encompasses an area larger than 1800 km² and shows also a local deformation at the Lastarria volcano affecting an area of around 50 km² (Figure 1d). A NNW - SSE profile crossing the deforming area allows us to compare the deformation rate of the two datasets (Figure 1e). We found that the mean deformation rate increased from the 1995 to 2006 (ERS) period to the 2003 to 2008 (ENVISAT) period, with a rate change from 1.8 to 3.2 cm/yr (Figure 1e). The profile also shows a short-wavelength signal with lower amplitude located at Lastarria (LAS). The observed displacement rate at LAS reaches up to 2 cm/yr from 2003 to 2008, with a part of this signal being related to the large-scale deformation field.

3.3 Source modeling

To quantify the sources responsible for the two-scale deformations, we invert the observed signal by applying a heuristic optimization method (Simulated Annealing), which follows the approach detailed by Kirkpatrick (1983). To isolate the displacement signal we first applied the linear Pearson correlation coefficient (Stanton, 2001) and searched for pixels that fell within 95% of a similar trend to the maximum displacement observation point (CEN) in Figure 1. Pixels that are not affected by the deformation are thus excluded. Second, we sub-sampled the cross-correlated dataset using a regularly spaced grid (1 km) that reduces significantly the computational time without affecting the parameter estimation performance. To evaluate a confidence interval for the estimated parameters, we iterated the inversion procedure 100 times and retained the models that fall within $\pm 5\%$ of the minimum cost (L^2 norm), assuming as best models the mean of parameters within this range. Because the main deformation scale is very

large and its source likely to be laterally extended (Ruch et al., 2008), we assumed an expanded dislocation plane acting as a sill source model (Okada, 1985), and then estimated its parameters. Although additional geophysical and geological data are missing to elaborate more realistic models, the models were performed in an elastic half-space medium with a Poisson's ratio $\nu=0.25$ and a Young's Modulus of $E=50$ GPa. The results suggest that the source depth for both datasets is located at 12-14 km below the

Table 1: Source parameter results using a rectangular dislocation plane (Okada, 1985). Inversion was performed for the long wavelength signal of the Lazufre area for both ERS and ENVISAT datasets.

LAZUFRE	ERS 1996-2000	ENVISAT 2003-2008
Length (km)	18.7 ± 0.2	21.3 ± 0.7
Width (km)	8.5 ± 0.9	6.7 ± 2.8
Depth (km)	11.8 ± 0.2	13.3 ± 0.3
Opening (cm)	5.1 ± 0.7	41.9 ± 1.0
ΔV source (km ³)	0.008 ± 0.0016	0.059 ± 0.001

surface and almost constant for the entire 13-year time series (see Table I). Residuals are generally less than 0.2 cm/yr with the exception of a near radial-symmetric deformation signal with uplift rates larger than 1 cm/yr centered on the Lastarria volcano (Figure 2a3-4) affecting an area of about 50 km².

We further investigated this residual deformation by applying a spherical source model approximation (McTigue, 1987). Because Lastarria is relatively steep-sided we also considered the topography (Williams & Wadge, 1998). The residuals are again generally less than 0.2 cm/yr, with the exception of the area where the three main fumarolic fields are located, which still shows a residual signal up to 0.5 cm/yr (Figure 2a6). We left the source position open, but constrained our model parameters to obtain pressure change values below a reasonable threshold of 10 MPa/yr, which is considered as a limit after which rock may begin to fracture (Manga & Brodsky, 2006). Our best fitting models

suggest a shallow spherical source, located between 0.6 and 0.9 kilometers below the Lastarria summit, in agreement with Froger *et al.* (2007). Although the deformation at Lastarria is a short-wavelength signal, we obtained similar shallow locations using other type of source model (Mogi, 1957). Therefore, because of the height of Lastarria volcano (1 km relative), the source appears to be located within the edifice. The source radius is ~ 0.3 km (between 230 and 360 meters) and subjected to a volume change of ~ 13000 m³/yr (between 8000 and 18000 m³/yr). The pressure change induced by the source is between 0.4 and 4 MPa/yr, cumulating in a range of 2 to 20 MPa over a five-year observation period (2003-2008). These values are compatible with the lithostatic stress values expected at such shallow depth.

3.4 Deformation starts and stress transfer modeling

We analyzed the time evolution of the local deformation observed at Lastarria volcano after the removal of the long wavelength signal caused by the deeper source (Figure 2b, LAS and LAS', respectively). Results suggest a temporal delay compared with the start of the broader inflation observed at Lazufre (CEN). Indeed, by assuming 1 cm accuracy to be a detection threshold, first evident deformation signal at CEN began in 1997 (marked by "A" in Figure 2b), while deformation at LAS' (marked by "B" in Figure 2b) was apparently not observed before the year 2000.

Numerical modeling may help to understand whether the stress field changes caused by the inflation of the deep source in the surrounding of Lastarria volcano can explain such delay. In our stress model calculations we quantified the change of

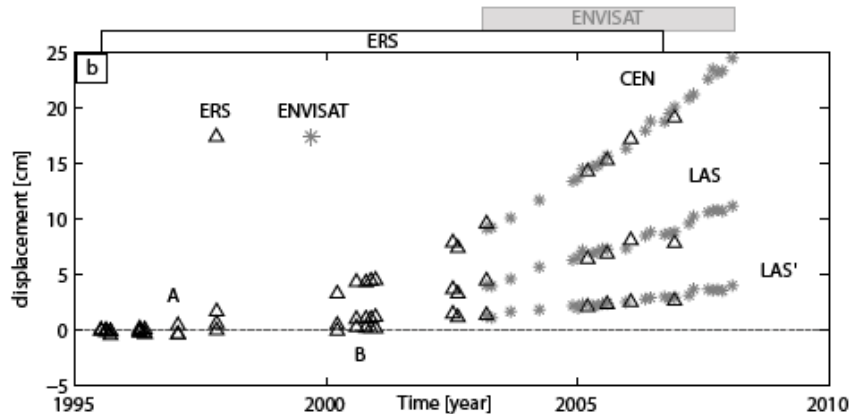
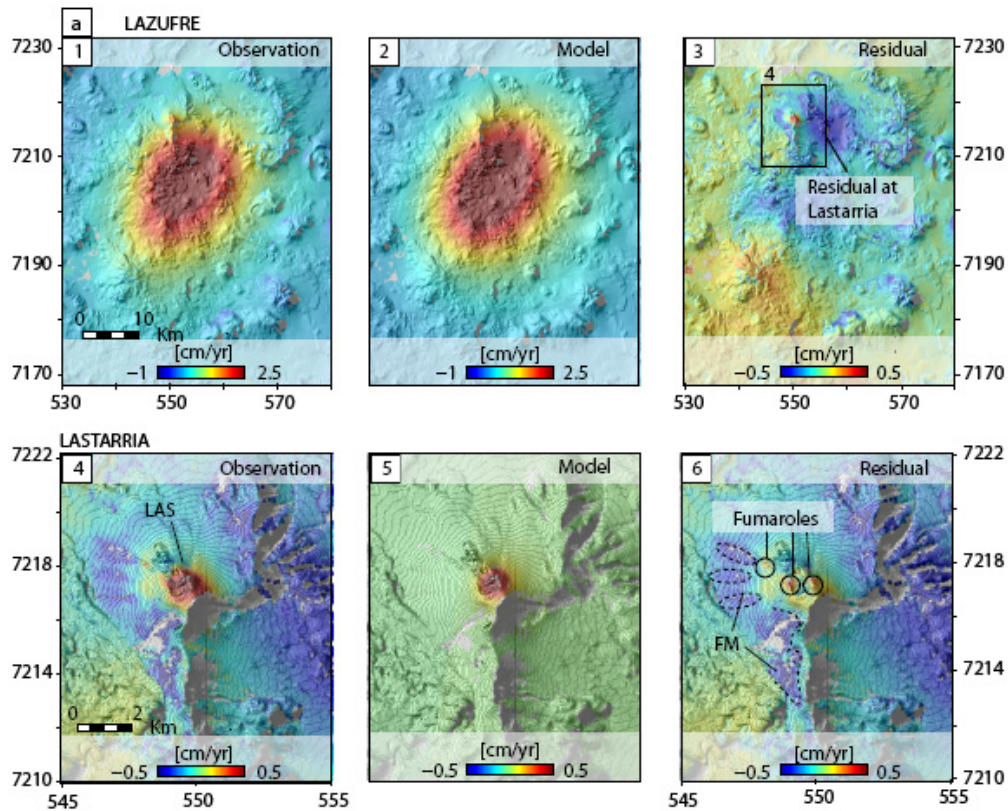


Figure 2: a) Inversion results of the Lazufre deformation data for the period from 2003 to 2008 (Table I). 1) Observation data, 2) synthetic models, and 3) residuals. Inversion of the Lastarria signal using a finite spherical source showing 4) the observation data, 5) the synthetic model, and 6) residuals that highlight the three main fumarolic areas (black circles). Dashed lines indicate flank movements (FM), which act on the western flank of the Lastarria volcano. b) The time series plot for the ERS (black triangle) and ENVISAT (grey stars) datasets for two observations points that correspond to both maximum displacements at Lazufre (CEN) and Lastarria (LAS). LAS' is plotted after removing the long wavelength signal to better assess the initiation of the deformation. Results show a two-year shift between both signals initiations at CEN (marked as A) and LAS' (marked as B).

the maximum tensile stress (σ_3), which is a common indicator for estimating occurrence and location of crack initiation (Anderson, 1951). Using a boundary element method (Thomas, 1993), we simulated the opening of the deep source by a dislocation plane for the period from 1996 to 2000 (Table 1). Because the influence of an active magmatic or hydrothermal reservoir can be approximated by a material property that is softer than the surrounding host rocks, we defined the shallow source as a void in an elastic medium (Savin, 1961). Therefore, we included a spherical source at shallow depth beneath the Lastarria summit and defined a free slip boundary condition that is able to open or close, simulating passive source inflation or deflation, respectively. Deformation of this inclusion perturbs the local stress field in the surrounding region. We found that close to

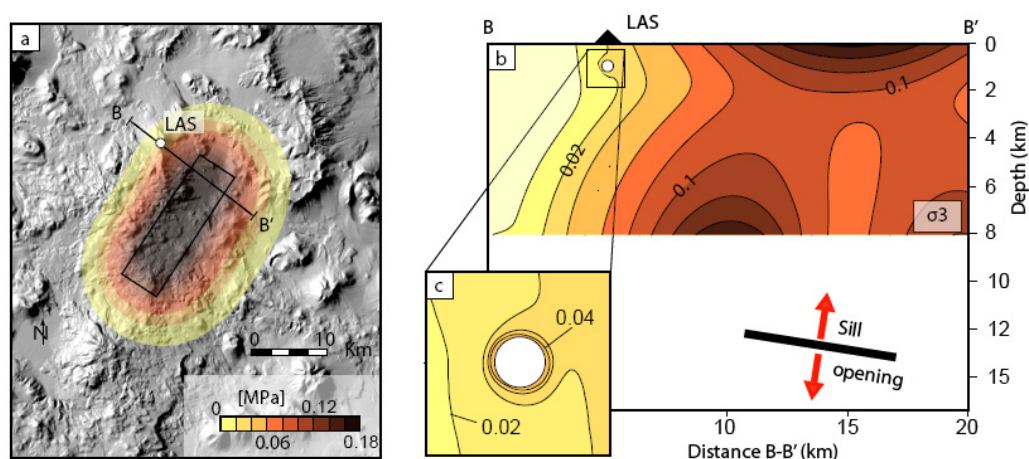


Figure 3: Stress transfer model at Lazufre for the period from 1997 to 2000. Maximum tensile stress σ_3 is caused in the area of interest by the deep source inflation a) at the surface. The black rectangle represents the best fit dislocation plane projected to the surface, b - c) Cross-section through B - B' that shows a slight increase of the tensile stress around the simulated source of Lastarria volcano.

the shallow source, the maximum tensile stress was more than twice as large if compared to a model without such an inclusion (Figure 3). For validation, we tested the stress field change using Finite Element Method with the same initial parameters and obtain similar results. The models implied that the inflating deep source caused the

maximum tensile stress at the shallow source to increase by 0.04 MPa between 1996 and 2000, before it displayed deformation above detection threshold. Until 2008, the induced stress change cumulated at around 0.2 MPa. Although these stress changes appear to be small, comparable values are thought to have triggered even volcanic eruptions elsewhere (Manga & Brodsky, 2006).

3.5 Discussion and conclusions

In the present paper, we used two InSAR datasets spanning the time interval 1995- 2008 to analyze multi-scale deformation patterns in the Lazufre volcanic area and test the relationship of neighboring volcanic systems. We analyzed the deformation signals through elastic half-space models, retrieving the location and volume change of the large-scale and small-scale sources. Using stress models, we tested the hypothesis that inflation of the deeper and larger source increased the tensile stress around the shallow source and may have even triggered the local activity at Lastarria.

Earthquake occurrences and volcano inflations have been proposed as triggering sources that modify the surrounding stress field and possibly reactivate dormant volcanoes. This was suggested to explain seismicity and fumarole activity at Long Valley (Hill et al., 2002) or even eruptions at Karymsky and Akademia Nauk volcanoes in 1996 (Walter, 2007). The amount of stress involved varies by several orders of magnitudes. Acidic dikes propagate at magmatic overpressures of up to 10 MPa, basaltic dikes at up to 1 MPa (Jellinek & DePaolo, 2003; McLeod & Tait, 1999), and may even initiate due to very small stress changes as induced by earthquakes of about 0.1 MPa or even below (Manga & Brodsky, 2006). Thus, small amounts of stress change, as calculated here in the surrounding of Lastarria volcano, may induce enough perturbation to encourage unrest. However, a volcanic or hydrothermal source needs to be in a critical stage to be

reactivated by small amounts of stress changes of about 0.1 MPa or below (Hill et al., 2002; Manga & Brodsky, 2006). Here, we estimate that 0.04 MPa accumulated prior to deformation starting at Lastarria and increased up to 0.2 MPa until 2008. This implies that the Lastarria volcano, which is strongly affected by hydrothermal and fumarolic activity, may have been in a critical stage susceptible to very small perturbations of the surrounding stress field, while other volcanoes located in areas where the induced stress changes are higher do not show any surface deformation.

Stress changes at a magmatic or hydrothermal reservoir may lead to a cascade of associated effects that are not yet fully understood. An extrinsic increase of the tensile stress around a void (magmatic or hydrothermal reservoir) might lower the pressure into it (Savin, 1961), generating a gradient that may in turn allow fluids or volatiles to migrate. The fluids might be trapped by the presence of a low-permeability cap that is known to partially seal active hydrothermal reservoirs at volcanoes (Aizawa et al., 2009). Comparable phenomenon was suggested to occur at other volcanic areas containing sealed hydrothermal system (Hurwitz et al., 2007). Stress changes at the reservoir walls may cause linkage of pre-existing fractures, thus leading to changes in rock permeability and encouraging fluid propagation (Wang, 2000). Therefore, the observed deformation at Lastarria may be the consequence of fluid-mechanical and rock mechanical processes.

The InSAR time series and stress models allow us to propose a possible relationship between two volcanic reservoirs. However, the models are simplified, assume a linear elastic material, and do not consider time dependent rheologies that may explain the delay between the two deformations (Wang, 2000). Material heterogeneities may affect part of the deformation signal, for instance, locally under the Lastarria volcano. Soft materials may amplify the surface deformation (Manconi et al., 2007). At Lastarria, soft material is present in the hydrothermally active regions (see Figure 1e), including the

intrusive core and the fumarolic field. The effect of material heterogeneity is also locally shown by the deformation residuals at the western flank of Lastarria volcano, where the retrieved LOS displacements are negative (see Figure 2a6). Our field inspection (Figure 1e) suggests that this locality matches the steep slopes $> 20^\circ$ of the volcano and consists of unconsolidated material, implying the signal is due to localized slow-flank movements or creeping phenomena. Unless studied in further detail, however, these contributors do not allow us to construct more realistic models, which would require additional geophysical information.

Therefore, our models suggest possible explanation of the processes occurring in the Lazufre volcanic area, as evidenced by the InSAR data analysis. Thus, we suggest that upward directed stress transfer occurs at Lastarria volcano, where changes of the shallow system may reflect an activity change at the deep source.

3.6 Acknowledgements

We acknowledge discussions with Maurizio Battaglia, Valérie Cayol, José Fernández, Jean-Luc Froger and Paul Lundgren. We are grateful to Matt Pritchard for his constructive comments, and for providing us with ERS images to extend our time series analysis. Envisat data were provided by the ESA as part of CAT-1 project # 3455. The research was partially funded by the DFG, grant # WA1642.

3.7 Auxilliary Material

The Auxilliary material contains two Figures regarding the atmospheric filtering applied on the Lazufre InSAR dataset, and 1 Figure that compares the topographic features and the deformation signals. Figure 3.7.1 contains an InSAR time series plot (ENVISAT dataset) with and without atmospheric filtering for two pixels located at both maximum

displacement at Lazufre and Lastarria. Figure 3.7.2 shows the Lazufre deformation map for the period 2003-2008 (total displacement) and the atmospheric residual. Figure 3.7.3 contains profiles across InSAR dataset and high topography features in the Lazufre area.

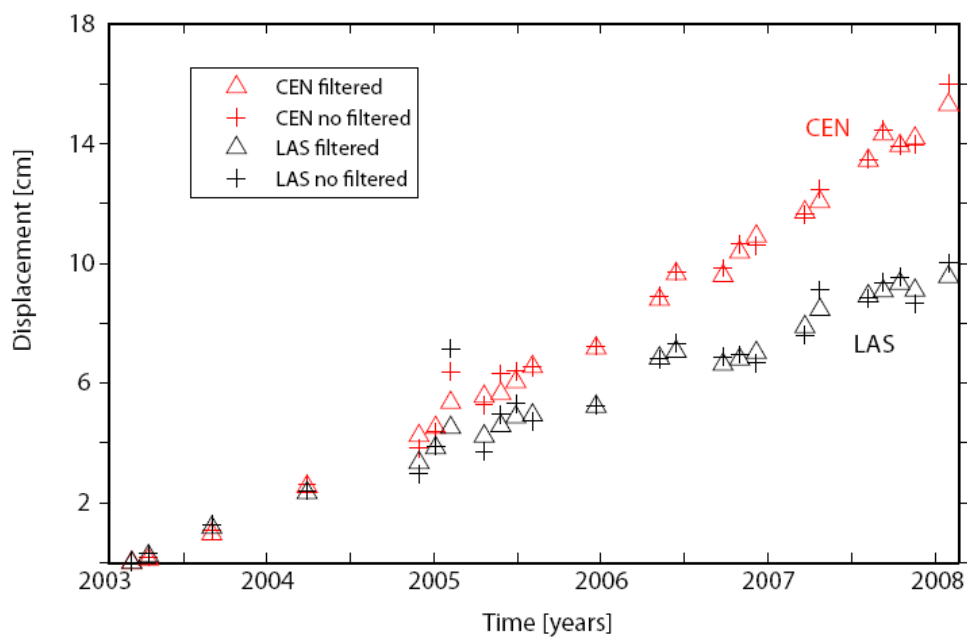


Figure 3.7.1: Two single observation points from InSAR time series corresponding to both maximum displacements at Lazufre (CEN) and Lastarria (LAS). Both are plotted with and without atmospheric filtering. Results show similarities between both analysis, with signal amplitude variations lying in the SBAS technique error.

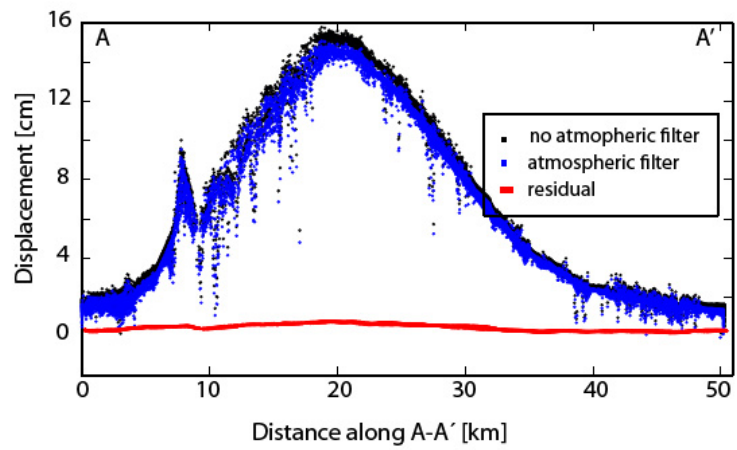
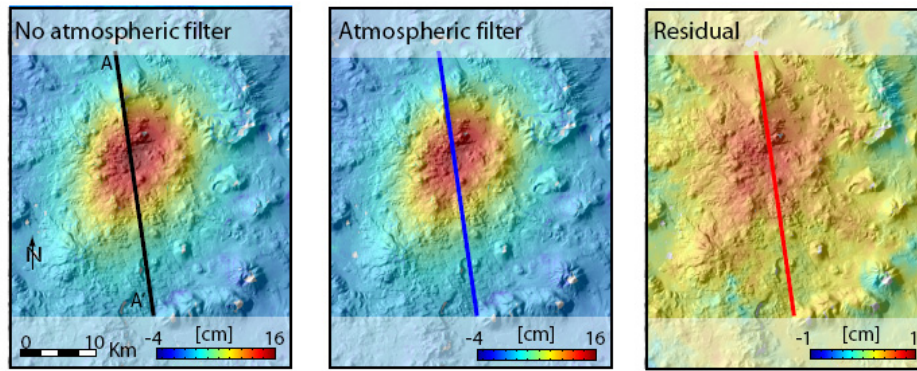


Figure 3.7.2: Deformation map of the Lazufre deformation for the period from 2003 to 2008 with and without atmospheric filtering. Note that residuals fall in the error bar of the SBAS technique.

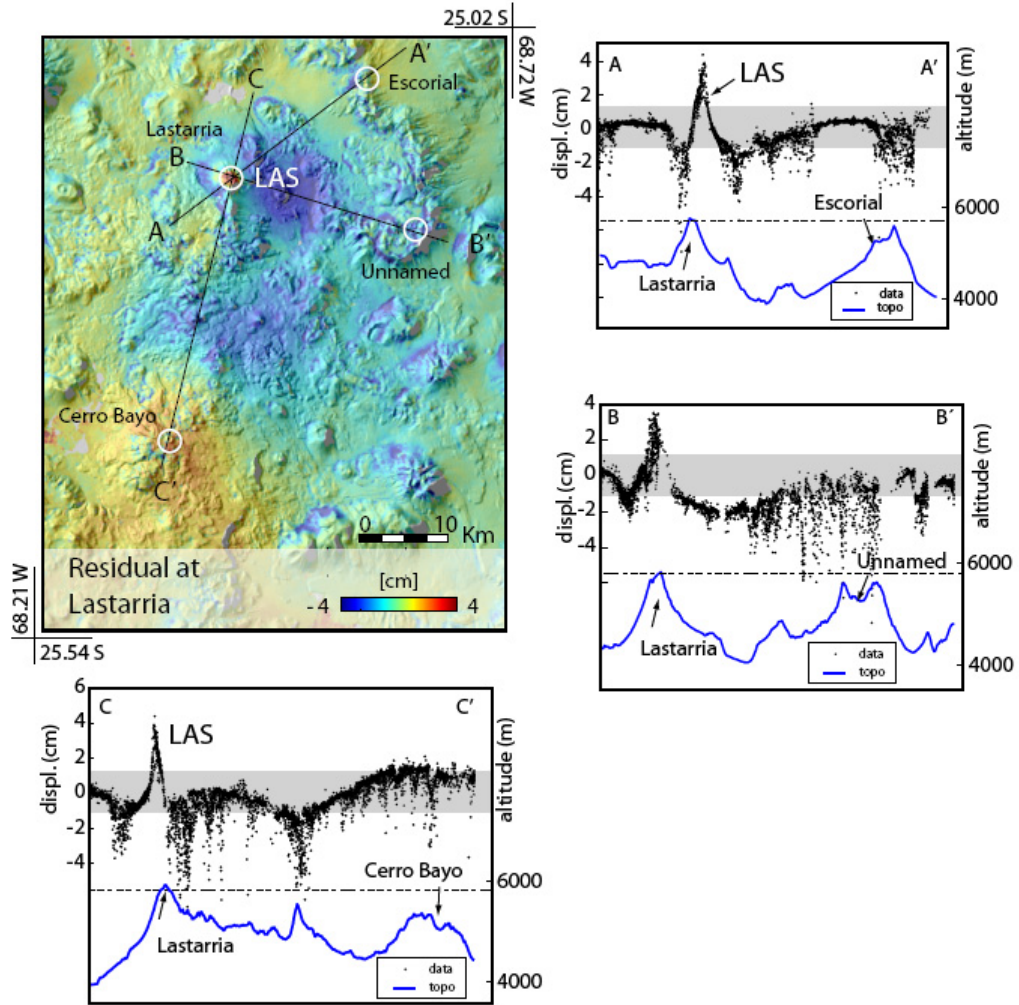


Figure 3.7.3: Profiles across the deformation dataset area plotted together with topography profiles at the same location (topo). If some artefacts due to topography or atmospheric effect were remaining, similar topographic features (volcanoes of same elevation) should show topography and signal correlations (artefacts). Results demonstrate that no systematic correlations of deformation signal with high topographic features are observed, thus the deformations observed are genuine.

Chapter 4

Relationship between current uplift geometry (InSAR) and the structural framework at Lazufre volcanic area, central Andes

J. Ruch^{1,2} & T.R. Walter¹

¹ GFZ, German Research Centre for Geosciences, Potsdam, Germany

²Dipartimento di Scienze Geologiche Roma Tre, Roma, Italy

Abstract

The stress regime and structural fabric in active tectonic areas controls the orientation of magmatic reservoirs and dikes. Hence volcanic structures provide potentially good indicators to assess the regional geodynamic processes through time. Here we analyse the spatiotemporal evolution of the Lazufre volcanic area in the central Andes, where a recent large-scale elliptical surface deformation was recently detected. Based on satellite radar interferometry (InSAR) the deformation signal is explained by a magmatic intrusion located approximately at 10 km depth. Herein we compare this elongated deformation with several volcanic structures around. We find that a higher concentration

of volcanic vents is located within the deforming area if compared to its surroundings. Furthermore, the mean orientation of volcanic structures is aligned in NNW-SSE direction (N129°), almost perpendicular to the mean elongation of the deformation ellipticity (N28°). Applying the borehole breakout concept we propose a unifying model that explains both short-term (InSAR) and long-term (volcano lineaments) magmatic activity by a similar stress field acting at depth of the intrusion and near surface alike. Important implications arise such as a temporal stability of the principal stress directions.

4.1 Introduction

Stress field acting at tectonically active margin is considered as a key component in the understanding of geodynamical processes through time. Eruptive fissures and vent orientations provide information about the stress field orientation at the time of the eruption, with dike intrusions striking parallel to the major horizontal compressive stress SH (Anderson, 1951; Nakamura, 1977a). Dikes, eruptive fissures and volcano lineaments consisting of faults, topography contrasts in volcanic areas are commonly used as stress indicators in different geodynamic contexts, as in the East African rift and in Iceland under extensive regimes (Acocella, 2002; Gudmundsson et al., 2006) and in subduction-related compressive and transtensional regime (Tibaldi, 2009).

In addition, volcanic areas are affected by large-scale surface deformations that have been recently detected by radar satellite technique (InSAR) and show deformations affecting areas larger than 1000km², considered as the surface expression of magmatic or hydrothermal reservoir acting at depth (Fialko and Simons, 2001; Pritchard and Simons 2002; Lundgren et al., 2006; Froger et al., 2007; Ruch et al., 2008; Annen, 2009; Anderssohn et al., 2009). Such reservoirs are generally described as weak intrusions that

have different mechanical properties compared with the surrounding rocks (Gudmundson et al., 2007). It is often proposed that their shapes are closely related to

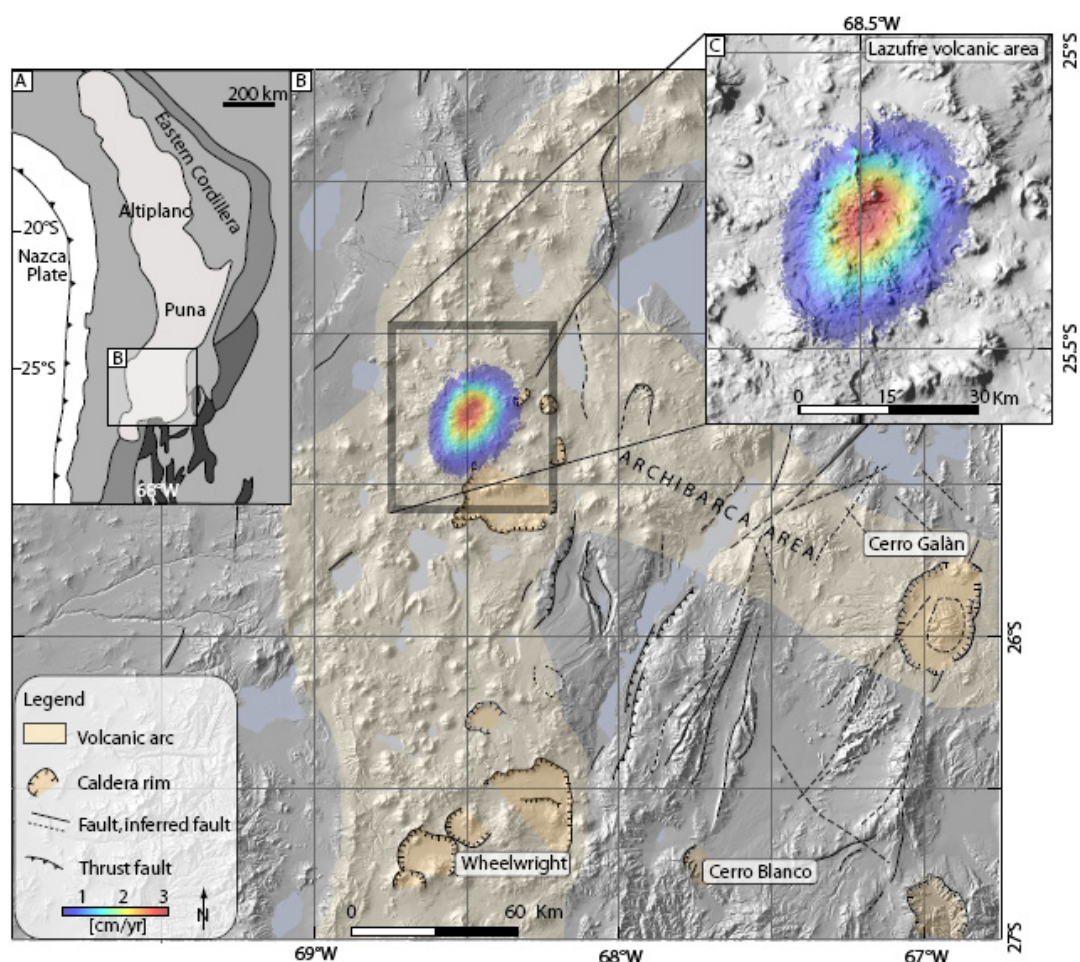


Figure 1. A) Simplified morphostructural map of the Central Andes (after Riller 2006), B) detail of the southernmost Puna plateau area that hosts the Lazufre deformation and large caldera structures such as Cerro Galàn, Wheelwright and Cero Blanco. C) InSAR observation details, with first sign of ground displacement detected in 1997, overlaid on a 90m DEM. Note the elliptic shape of the deformation that strikes in NNE-SSW direction.

the regional stress acting on their walls, with preferential reservoir elongations perpendicular to the principal horizontal stress SH (Bosworth et al., 2003). Alternatively, such intrusions may use pre-existing tectonic structures that facilitate reservoir expansion through time (Acocella et al., 2002).

Here we test the agreement and relationships of volcanic structures as dike and eruptive fissure emplacements with a recent elliptic deformation detected by InSAR in the Lazufre volcanic area (central Andes).

4.1.1 Volcano-tectonic context

The Lazufre volcanic area (Pritchard and Simons, 2002) is located in the central Andes about 300 km far from the trench where the Nazca plate subducts beneath the South American plate. The compressive regime acting at this convergent plate boundary gave rise to the actual high elevated Altiplano Puna plateau (Oncken et al., 2006 and references therein). Lazufre is part of the southernmost Puna plateau (Figure 1A) with heights over 4000 meters and is located at an intersection between the actual volcanic arc and the northwest regional trending Archibarca structural corridor. Archibarca appears to control the localization of magmatism and hydrothermal ore deposits products and the related lineaments are interpreted as deep-seated basement structures (Richards and Villeneuve, 2002).

Major caldera volcanism has occurred in the region during the Late Miocene-Pliocene (de Silva and Francis, 1991). To the southeast is located the Cerro Galàn caldera, the youngest in age in the central Andes (2Ma), which is structurally elongated in NNE-SSW direction (Holohan et al., 2005). In the south is located the Wheelwright caldera complex composed of three nested depression structures, forming a nested structure oriented in NE-SW direction, and the Cerro Blanco caldera system, that follows a similar structural orientation (Figure 1B).

In this area, Lazufre is currently the only volcanic system that shows signs of unrest with the exception of Cerro Blanco (Pritchard and Simons, 2002). Although Lazufre is not a caldera, it is comparable in size with caldera systems. At Lazufre are observed two time span volcanic activities; a 10^1 years recent and large-scale surface deformation that

affects Pleistocene (10^5 years) volcanic products. Lazufre comprises three high elevated stratovolcanoes located above 5000m and numerous volcanic vents (Figure 1C). The Lastarria volcanic complex (5700m asl), which is made of various morphostructural components (Naranjo, 1992), included the southern spur with older volcanic products with respect to the nested summit craters located northward. Although no historical eruption has been reported there (de Silva and Francis, 1991; Naranjo, 1992), strong and persistent fumarolic activity occurs at the summit region (Naranjo, 1985). Other known volcanic centres of the Lazufre area are the Cordon del Azufre and the Cerro Bayo volcanoes, both Quaternary in age that form a series of craters and associated lava flows located in the central and southern region (De Silva and Francis, 1991). Lazufre is covered by Pleistocene or younger volcanic material, overlaying generally Tertiary volcanics (Naranjo and Cornejo, 1992; Trumbull et al., 1999).

First sign of ground displacement (uplift) was detected at Lazufre using radar interferometry (InSAR) in 1997 by Pritchard and Simons (2002). Consecutive studies show a deformation rate up to 3 cm/yr (Froger et al., 2007; Ruch et al., 2008, Anderssohn et al., 2009), affecting an area larger than 1800 km² in 2008 (Ruch et al., 2009). Source depth estimations are between 9 and 17 km depth (Pritchard and Simons, 2002). Almost three years after the Lazufre uplift initiated, a second, smaller deformation of 50km² was detected on its northern margin on the main Lastarria craters with deformation rate up to 1.5 cm/yr (Froger et al., 2007; Ruch et al., 2009).

4.2 Recent deformation and structural framework analysis

To test a possible relationship between the current inflation geometry and the structural framework, we analyse the geological and structural context of the Lazufre volcanic area, evaluating the respective structural and geometrical orientations. We used on one

hand InSAR observations acquired by the ENVISAT satellite for the period from 2003 to 2008. On the other hand we mapped out Pleistocene volcanic structures using both 90m and 30m resolution Digital Elevation Model (DEM) from the German Aerospace Center, multispectral Landsat images with a 15m spatial resolution, as well as a set of 21 geo-referenced aerial photographs that partially cover the area of interest (*flight 18 1020-1010; flight 32, 2744-2753 of the Military Geographic Institute, Chile*). We thus combined and analysed the current deformation and the Quaternary structures under a GIS platform (ESRI, 2008).

4.2.1 Deformation geometry detected by InSAR

InSAR techniques compute the phase difference (interferogram) between temporally separated SAR image pairs to obtain an estimate of the ground deformation projection in the radar sensor's line-of-sight (Massonet and Feigl, 1998). We use in this study an InSAR time series dataset acquired by the ENVISAT satellite made of 21 subsets spanning from March 2003 to January 2008 (see details in Ruch et al., 2009). We completed a cross correlation analysis of the deformation for the entire period, to identify pixels moving synchronously with respect to the maximum uplifting area. For our analysis, we have computed the linear Pearson correlation coefficient (Stanton, 2001) over the whole dataset. We retain data with a correlation value >0.95 , thus, signals which are not directly correlated to the deformation are not considered. As a result we observe a constant elliptic deformation pattern for a period spanning almost 5 years (see Figure 1C).

We fit the cross correlated observation mean velocity pixels with an ellipse using a linear least square approach (Gander et al., 1994), then assumed its mean major axis as representative of the mean deformation orientation, striking at N028. For consistency, we analyze in details the deformation geometry evolution of each of the 21 subset from

2003 to 2008 and found similar orientation results striking at $N028\pm 2$. Source characterizations obtained by inverting the Lazufre signal using a dislocation plane (Okada, 1985) that acts as a sill opening at depth strikes in $N030\pm 2$ direction (Ruch et al., 2009). To compare the orientation of the deformation with the volcanic structures orientations, we thus analyze the volcano lineaments located inside and around the deforming area.

4.2.2 Volcanic structures analysis

To analyze precise location and orientation of volcanic features and related dikes, we used a methodology based on established morphometric parameters as volcanic vent elongations, eruptive fissure orientations and fault across volcanic vents (Nakamura, 1977a; Tibaldi, 1995).

We considered and mapped lineaments when it shows 1) a density higher than 1.5 vents/10km², 2) a clear topography-related ridge resulting from vent emplacements, 3) the presence of elongated craters. For consistency, we considered only the dated volcanic edifices or those that are build on dated volcanic series younger than Pleistocene (Naranjo and Cornejo, 1992; Trumbull et al., 1999). Our results show that the Lazufre area contains more than 100 vents, with a spatial density higher inside the deforming area compared to the surroundings. We obtained values up to 5.6 vents/10km² coinciding with the central area of the deformation detected by INSAR, forming a semi-crowned shape morphology (Figure 2A), with vent types mainly represented by monogenetic edifices. We thus mapped out volcano lineaments and eruptive fissures in areas where feeding dikes orientation may be estimated. Details of selected lineaments are illustrated in Figure 2B-D. The Lastarria volcano shows five distinct nested craters

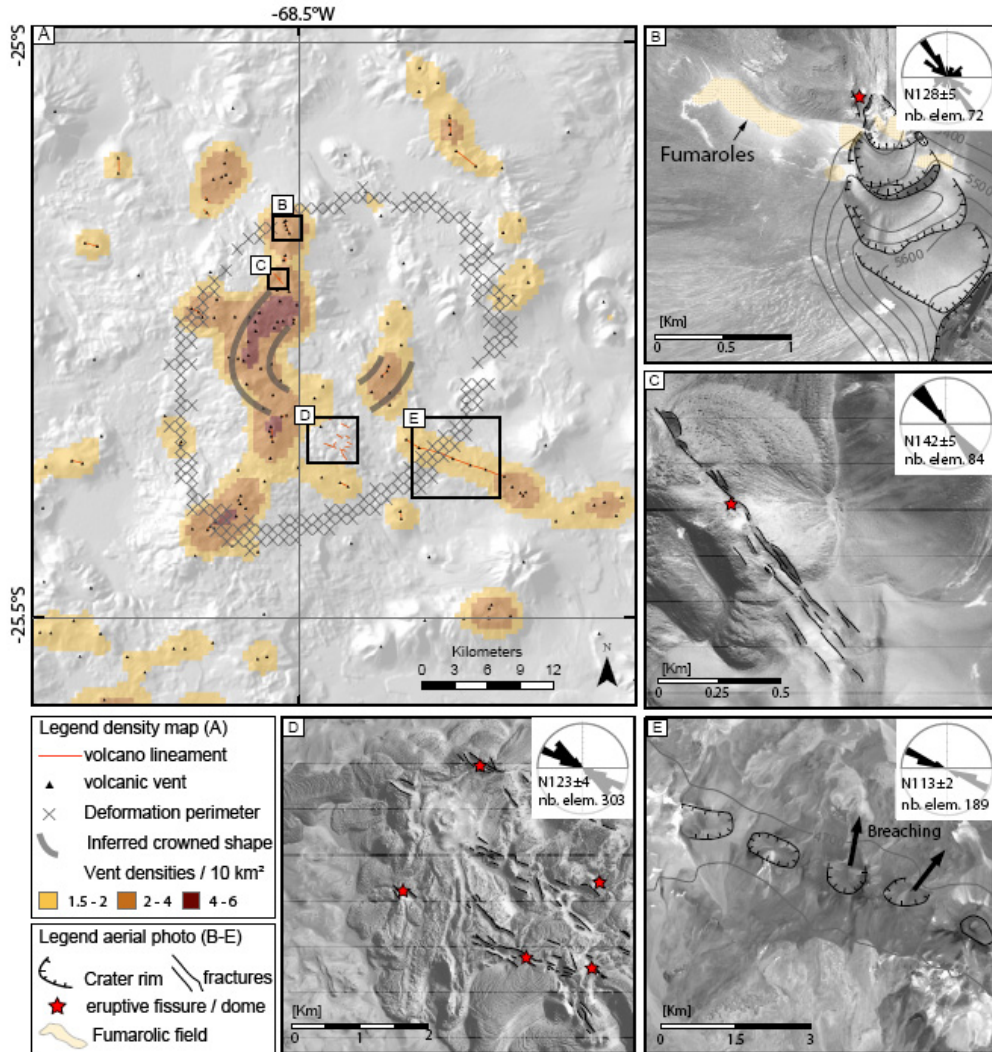


Figure 2. A) Volcanic vent density map at Lazufre. Black boxes indicate the volcanic structures detailed in the four subsets. Note the highest vent density inside the deformation perimeter that formed a semi-annular shape morphology. Structural maps overlaid on orthophotos for B) the five Lastarria nested craters with a NNW trend orientation. Topographic lines are marking each 50m, in light grey C) the Negriales lava field with cracks oriented at N128 direction, D) a 8 km wide, 10 km long eruptive fissure composed of several cracks that emitted thick dacitic lava flows, with mean orientations striking N120, E) an eruptive fissure of 10 km long and 0.5 km high that shows a clear N128 orientation. Rose diagrams illustrate the mean lineament orientation subdivided by sectors of 10°.

extending in a 2km long NNW-SSE segment in the major axis with a mean strike of N128±5 (Figure 2B). At the south western part of Lastarria is located the Negriales eruptive fissure that was emitted earlier than Lastarria (Naranjo, 1992). The fractures show an orientation striking N142±5 (Figure 2C). Note that this lava field follows a

similar orientation than an older longitudinal depression zone that may imply a reuse of pre-existing structures. Another example of a close-up view is shown in Figure 2D by fissure zone covering an area of about 25 km², with fracture lengths ranging from few meters up to 0.5 km oriented at N123±4°. The cracks were associated with emissions of thick dacitic lava flows (de Silva and Francis, 1991). The lava field covers an almost flat area, without strong signs of ground topography variations. Finally, we observed in the south eastern part a clear 10km-long high topography ridge with two NW-SE elongated craters, and 2 vents breaching that strike toward the NE, almost perpendicular to the topographic axis (Figure 2E). In this case, a combination of vent elongation, vent breaching located on a clear topographic ridge allowed us to estimate the lineament orientation striking in N113±2 direction. By averaging the volcano lineament and eruptive fissure orientations we obtained a mean orientation striking in N129±7 direction.

4.2.3 Volcano lineament and volcano deformation as stress field indicators

Associating the ellipticity of the Lazufre deformation evidenced by InSAR and the volcano lineament observations, we found that they strike almost perpendicularly at N28±2 and N129±7, respectively (Figure 3C). Following Bosworth et al. (2003), we present in the following a simple conceptual model that may explain both orthogonally-oriented structures by a unique stress field orientation.

Large magmatic reservoirs, considered as soft intrusions in the upper crust, for simplicity may be considered as cavities surrounded by crustal rocks (Savin, 1960). By

mechanical analogy to the formation of breakouts in boreholes and tunnels, such

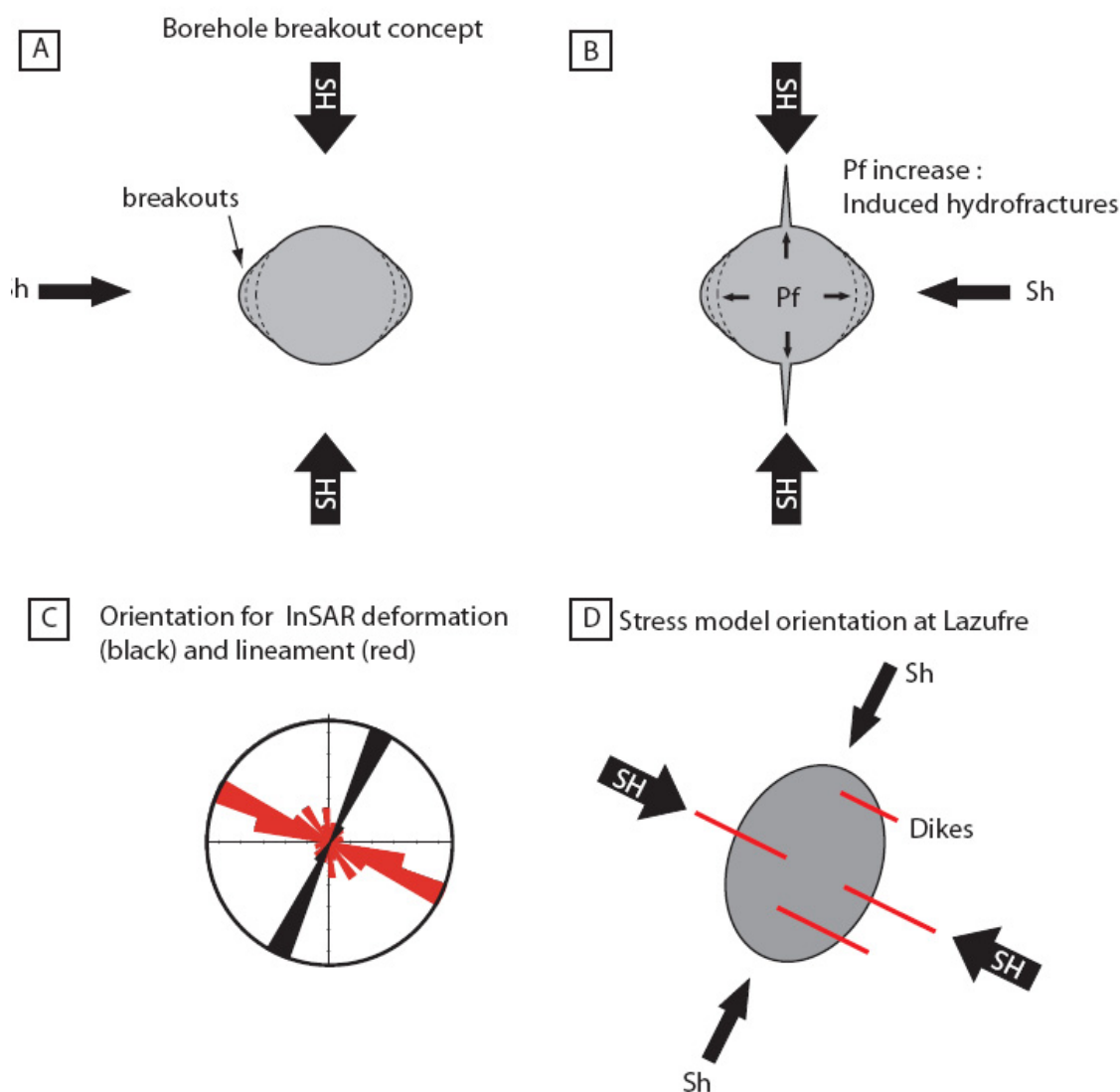


Figure 3. Borehole breakouts concept applied to the Lazufre volcanic area. A) Borehole subjects to an external stress field, with walls breaking perpendicularly to the maximum horizontal principal stress (SH ; after Bosworth et al., 2003), B) Same as A) with additional internal fluid pressure (P_f) increase, inducing hydrofractures that propagate parallel to SH , following the Anderson's theory (Anderson, 1953). C) Rose diagram that combine both InSAR observations (black) and volcano lineaments (red) show orthogonal orientations. D) Borehole breakout model applied to Lazufre. The reservoir will propagate and be elongated along the minimum horizontal compressive stress (Sh); dikes may propagate perpendicularly to the ellipticity due to pressure increase inside the reservoir that may trigger in turn volcano lineaments observable at the surface.

reservoirs may become elliptic perpendicular to the maximum compressive horizontal stress SH (Figure 3A) by stress-induced breaking of their chamber walls (Bosworth et al., 2003). Thus, if the pressure inside the reservoir overcomes the strength of the

surrounding material, hydrofractures (dikes) may propagate parallel to SH (Figure 3B) (Kirsch, 1898). Figure 3D shows a simplified compilation of our results that explains both orientations by a unique stress field being constant in depth and time. This has important implications for the geodynamic evolution understanding of the central Andes and similar mountain building processes elsewhere.

4.3 Discussion

In this study we analyze a large-scale volcanic deformation evidenced by InSAR and compare it with the geologic and tectonic surroundings. By comparing both volcanic activities we show 1) that the deforming area contains a higher vent density compared to its surroundings, and 2) that the deformation area is elliptical and strikes almost perpendicularly to Pleistocene and younger volcano lineaments. We further propose a temporal and spatial relationship between these two independent observations that may be considered as complementary stress indicators in the volcanic arc from the Pleistocene to the present day.

Although mainly based on morphostructural evidences, also other recent studies propose ellipticity as a stress indicator, as observed at Yellowstone caldera with the associated orthogonal Inio dikes, at Long Valley, or in the east African and Icelandic rifts (Bosworth et al., 2003; Holohan et al., 2005). Similarly at Novarupta in Alaska (Wallmann et al., 1990), at the Nirano hydrothermal area in Tuscany (Bonini, 2008), as well as in the West Antarctic rift system (Paulsen and Wilson, 2007). Here we apply the concept proposed by Bosworth et al. (2003) to explain large-scale deformation ellipticity. We study the Lazufre deformation that we suggest to be the surface expression of a magmatic system evolving at depth. Our results are consistent with other independent observations that suggest a similar stress field orientation observed in

adjacent area. Recently, Tibaldi et al. (2009) observed in the Atacama region (250 km north from Lazufre) that major normal faults and dikes are oriented accordingly to our results with a *SH* oriented in NE-SW direction. At a regional scale, some indicators of the world stress map and recent boreholes analysis on the eastern cordillera show also comparable *SH* orientations (<http://dc-app3-14.gfz-potsdam.de/>).

Alternatively, elliptic calderas are proposed to be the consequence of pre-existing structure reactivation that may be used as a pathway for magma to ascent at the time of the reservoir growth (Acocella et al., 2002). Figure 1 shows several regional lineaments that strike in an orientation similar to the Lazufre ellipticity and may hence imply a potential relationship between pre-existing structures and volcanism. However, the lack of structural studies in this area does not allow us to constrain the type and subsurface faulting geometry and its recent activity.

We assume the Lazufre deformation as representative of the reservoir geometry at depth, however, analogue model of caldera structures suggest that in certain cases elliptic structures observed at the surface may also result from a spherical source inflating located at depth, depending on the differential stress acting at depth and at the surface alike (Holohan et al., 2005). Although our results suggest a similar stress field orientation, complementary ongoing geophysical studies as seismic tomography may ameliorate our understanding about the source geometry.

At Lazufre, different volcano types took place during different time span. Dike and eruptive fissure emplacements are fast (<10 years), whereas composite volcanoes take place over longer periods (10^5 years). In our analysis we give a similar weight for both types. We believe this will not modify the consistency of our results. Fast emplacement of volcanic features are considered as clear stress field indicator, taking place in a very brief period, whereas composite and high elevated volcanoes (> 1000m from the volcano base) may have locally modified the stress field under their own load.

Although part of our results bring new and complementary information about the regional stress field in the volcanic arc, some structural evidences suggest that a local stress field may exist, in relation with a magmatic reservoir evolving at depth. Pritchard and Simons (2002) observed a crowned morphology composed of volcanic centres surrounding a central topography depression that is spatially correlated with the maximum uplift signal of the deformation. Our vent density analysis shows this in details illustrated by a semi-circular morphology essentially composed of monogenetic volcanoes (see Figure 2A). This is in good agreement with dome-like analogue models induced by an inflating source at depth that show tensional circular shape at the surface (Roche et al., 2000).

The stress regime in the Altiplano-Puna plateau is studied in detail in areas adjacent to the volcanic arc, where compressive regime is dominant (Allmendinger, 1997). For instance, the mean stress field orientation in the Eastern Cordillera (see Figure 1A) obtained by crustal seismicity and geological observation shows a regional shortening trend striking NNW-SSE (Coutand et al., 2001 and references therein). However, numerical models of intraplate stress fields including topography and the compensate crustal root effects, suggest a transition from compressive to transtensive and extensive regimes at elevations higher than 3 km above sea level with the maximum tension direction being oriented normal to the mountain range (Meijer et al., 1997). In this case, the principal stress σ_1 , which has a horizontal component in compressive regime at low elevation will gradually be shifted to the vertical in response to the Andean load compensation. This may induce transtensive and extensive regime in high mountain range, whereas the maximum horizontal compressive stress SH will remain in a constant orientation. This may explain that our results suggest a similar SH orientation at 10 km depth and at the surface alike.

4.4 Conclusion

In this study we combine independent information issued from a volcanic deformation observed by InSAR, together with volcanic structures. We find that both observations may be used as complementary proxies to assess the stress field orientation and the geodynamical context in areas where no strong structural evidences are observed.

4.5 Acknowledgements

We acknowledge Manfred Strecker and Oliver Heidbach for fruitful discussions and Bob Trumbull for earlier conversation. Funding was provided by DFG (Wa 1642/1-4) and by GFZ Potsdam for a field expedition in 2008.

Chapter 5

Salt lake growth detected from space

J. Ruch^{1,4}, J.K., Warren², F. Risacher³, T. Walter⁴, R. Lanari⁵

¹ Dipartimento de Scienze Geologiche, Roma Tre, Roma, Italy

² Faculty of Science, Chulalongkorn University, Bangkok, Thailand

³ IRD - CNRS Laboratoire d'Hydrologie et de Géochimie de Strasbourg, France

⁴ Helmholtz Institute, GeoForschungsZentrum, Potsdam, Germany

⁵ IREA, Centro Nazionale di Ricerca (CNR), Napoli, Italy

Abstract

Although salars are sensitive to environmental changes, analysing and understanding their hydrologic behaviour through time may contribute to monitoring actual and future climatic variations. Using a time series dataset acquired by satellite radar interferometry technique (InSAR) for the period from 2003 to 2008, we investigate the spatiotemporal evolution of salars in the Altiplano of the central Andes. We find that all salars surveyed are actively deforming, with displacement rates from 0.25 to 1.3 cm/yr. The deformation signal is generally linearly increasing in time and is confined to the salar itself, delimited by stable surroundings, with rates greater in some areas of some salars. To understand why, we further compare these observations of variable deformation rates with optical images acquired by the Landsat satellite, ground photographs and with in situ geochemical measurements of water brines sampled at the salar surfaces. We find direct correlations between these observations

and infer that the most rapid regions of salar deformation (rise) indicate active zones of vertical accretion, driven by capillary halite precipitation. We further propose that salars, whose dynamics are dependent on the presence of water and resurging saline groundwater, may be used as potential indicators of water resource evolution in the central Andes. To our knowledge this the first time the effects of salt precipitation processes on the rates of elevation change of salar surfaces have been quantified and related to broad scale facies associations and to economic potential.

5.1 Climatic and sedimentologic framework

During the Mid-Holocene period the Altiplano Puna plateau underwent rapid regional climatic change, shifting from vegetated areas subject to frequent rainfall to a more inhospitable desertic environment (Betancourt et al., 2000; Núñez et al., 2002). In response to the desertification, lake levels decreased from 8 to 3ky BP and many former perennial lakes desiccated into salars. The term salar describes salt-encrusted flats formed by the evaporation of flat-surface or shallow subsurface groundwater discharge in hydrographically closed (endoreic) desert depressions (Figure 1b). Across much of its extent, the Altiplano Puna encompasses substantial portions of the hyperarid Atacama Desert, one of the driest regions of the world (Figure 1a, Strecker et al 2007), with an average elevation of 3750 m.

Within a salar, there are a number of typical sedimentary sub-environments tied to inherent hydrological characteristics and responses to the evaporation of shallow near-surface and surface waters. At the broadest scale, the salar sediment system consists of two parts: a halite nucleus and a marginal zone (Figure 1c-d) with respective proportions

varying from one salar to another. Compared to the marginal zone, the halite nucleus surface is typically a zone of somewhat higher elevation in the salar plain. The salty surface of the halite nucleus facies association is typically irregular and jagged, and is composed of mm-scale sugary inclusion-poor halite crystals and eolian silts (Figure 1c). Nucleus halite forms in a halite-saturated hydrology, dominated by evaporation, capillary wicking and occasional episodes of rainfall-driven meteoric dissolution (Bobst et al., 2001). The halite nucleus facies association defines a brine sump in a salar and so

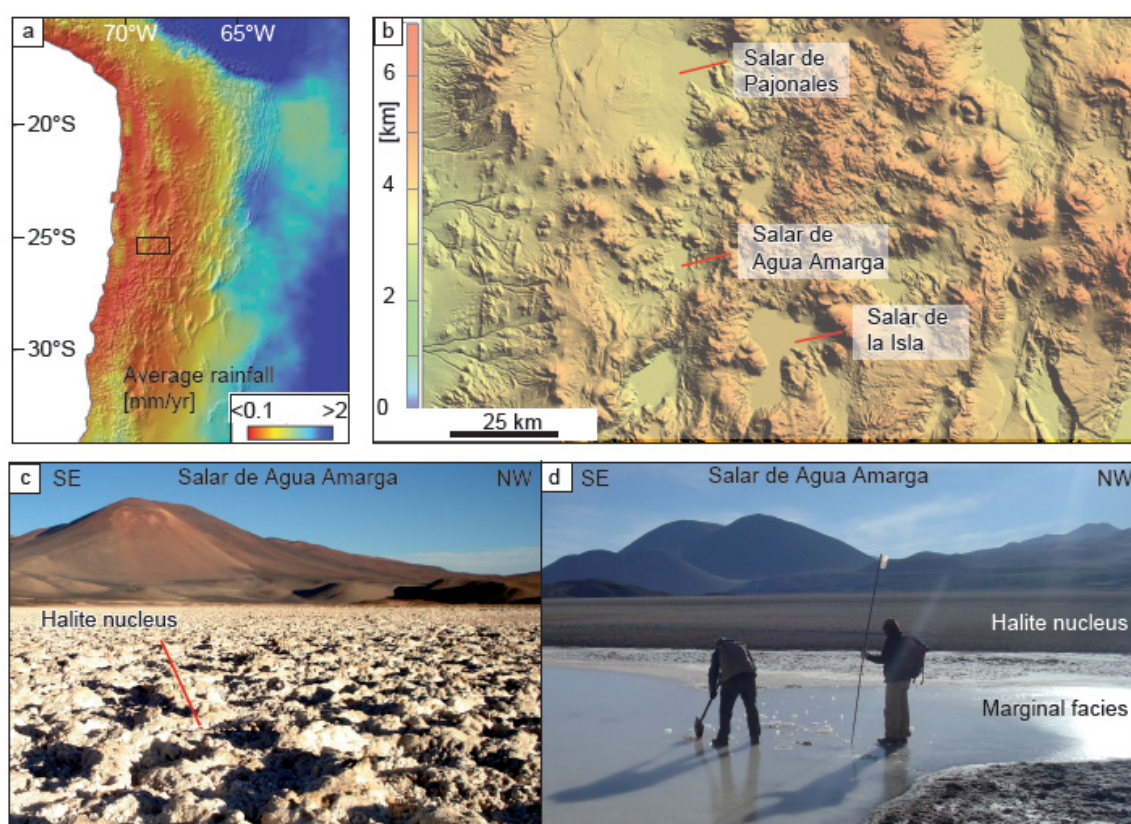


Figure 1: Salar locations. a) Topographic base map of the central Andes overlain by annual rainfall (modified from Strecker et al., 2007). Rectangle indicates the position of study area. b) Digital elevation model of the South Puna Plateau. Surface geology of Salar de Amarga that shows c) irregular surface of the halite nucleus facies and d) flat surface of marginal facies in south.

indicates a relatively stable hypersaline hydrologic setting that, in combination with a long-term brine feed, allows evaporitic sediment to accumulate and be preserved.

The surfaces of the adjacent marginal facies are varying combinations of silty mudflats, saline pan crusts, brine ponds and salty efflorescences (Figure 1d). Sheet flood and alluvial processes supply much of the terrigenous mud and silt sediment found in the fringe zone. The marginal facies association has a somewhat lower surface elevation when adjacent to the capillary crust region of the halite nucleus, with height differences ranging from tens of centimetres to more than a metre. Spring-fed lakes and brine pools (lagunas) are typically interspersed within the marginal facies association in most Andean salars. Marginal facies sediments are more liable to be covered by occasional floodwater, which drive the partial to complete formation of re-resolution crusts, and so do not offer such a stable hydrological setting as the halite nucleus sump. Surface evaporation rates are higher in the marginal facies associations compared to the halite nucleus even though the phreatic surface is typically shallow a few cm to tens of cm below the ground surface in both (Tejeda et al., 2003; Houston et al., 2006).

5.2 Deformation measurements

To analyse surface deformation in the zone of interest, we use an InSAR dataset acquired by the Envisat satellite composed of 21 images in descending orbit (track 282, frame 4118) spanning from March 2003 to January 2008 (Figure 1 on DEM). By processing the phase difference (interferogram) between SAR image pairs separated in time, we obtain temporal and spatial surface displacement projected along the satellite line-of sight (LOS). We applied the SBAS algorithm (Berardino et al., 2002) to obtain mean deformation velocity maps and time series with average standard deviation of 0.1 - 0.2 cm/yr and 0.5 - 1 cm (Casu et al., 2006), respectively.

Regionally, we observed a total of 12 deforming salars of different sizes, all showing clear displacement gradients, typically beginning in the uppermost salar shorezone,

landward of which the ground displacement is negligible (Figure 2). Locally, we

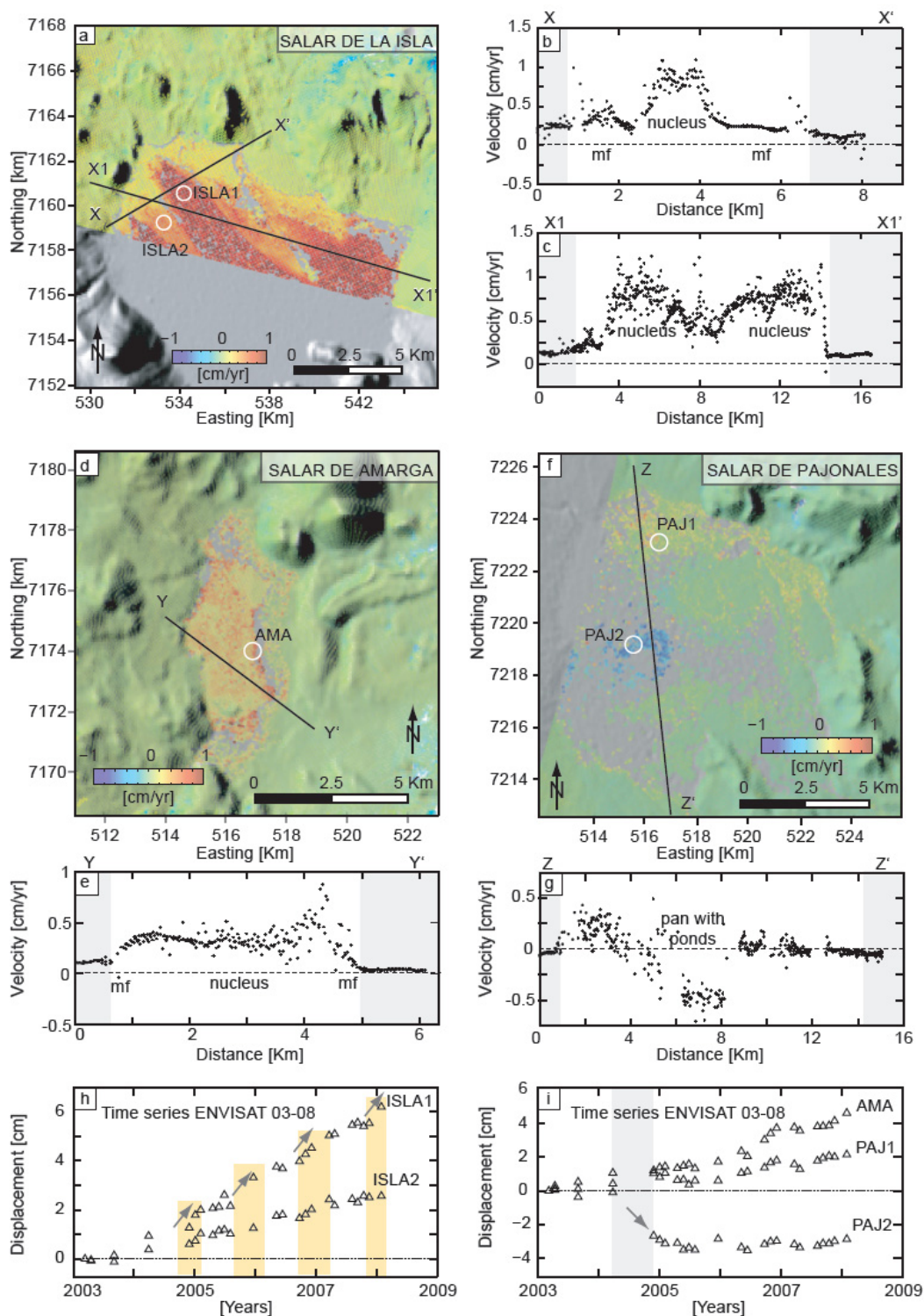


Figure 2. Deformation maps acquired by InSAR during the period from 2003 to 2008 on a DEM at a) salar de la Isla with b) and c) are profiles across the velocity map. d) Salar de Agua Amarga and e) velocity profile across the InSAR dataset. f) Salar de Pajonales with g) velocity profiles across the InSAR dataset. All profile transects are black lines on the deformation map and the grey bars notice the shore of the salars on the velocity

profile plots; mf: marginal facies. h) Time series plot at salar de Isla, with orange rectangle and grey arrows point out possible seasonal acceleration phases well visible at ISLA1, i) time series at salar de Pajonales and salar de Amarga.

conducted more detailed analyses on three salars (Salar de la Isla, Salar de Agua Amarga and Salar de Pajonales) that illustrate diverse relative proportions of surface facies, deformation types and rates.

The northern portion of Salar de la Isla has a maximum vertical displacement rate twice that of the other salars during the period of observation. Within the Salar de la Isla, two different rates are clearly observed at the salar surface (Figure 2a) and along the velocity profiles (Figure 2, profiles X-X' and X1-X1') with velocities from 0.5 up to 1.2 cm/yr. These profiles show clear acceleration transitions from the shore into the salar, with the strongest gradient observed across the halite nucleus facies association on the profile X1-X1' at km 14.5, transiting from 0 on the volcanic surrounds to around 1.25 cm/yr atop the halite nucleus, across a lateral distance of few hundred meters.

In Salar de Agua Amarga, a transition from shore into the salar is also evident, and we observe 2 groupings of deformation rates, from <0.5 cm/yr atop the halite nucleus near the geographic salar centre, up to 1cm/yr at km 4 on the profile YY'. This latter position on the transect intersects part of a broader circumferential perimeter to the nucleus showing higher deformation velocities (Figure 3b). It corresponds to the sedimentary boundary between the marginal flat facies and the halite nucleus facies associations in the salar that suggests an active hydrologic recycling of solutes along the eastern side of the salar. Overall the halite nucleus surface is not rising as fast in this salar as in Salar de la Isla.

Portions of all three salars surveyed in this area show some evidence of surface uplift or aggradation (Figure 2a-g); the central and southern parts of Salar de Pajonales are different. There, the deformation signal is locally negative, and forms an annular-shaped

geometry (Figure 2f). The velocity profile ZZ' shows from the north to the south, a transition from 0.5 cm/yr to -0.5 cm/yr. This salar lacks a halite nucleus and has a surface characterised by dissolution lagoons and ponds, interspersed with saline pan crusts. This association of degradation of the salar surface, and the presence of a marginal facies equivalents with abundant evidence of dissolution (Figure 2g) suggest saline sediment in this endoreic salar depression is being lost at a relatively high rate by passage of solutes into the regional groundwater system. Interestingly, this salar has the least hydrographic closure and is the only salar of the three studied that is juxtaposed to a huge bajada complex on western side of the salar (Figure 1b).

To better appreciate the temporal evolution of the salar surface, we compiled displacement time series on selected areas from 2003 to 2008. ISL1 (atop halite nucleus) and ISL2 (atop saline pan) are both located at the northern end of salar de la Isla (Figure 2a-c). They show different cumulative displacements sampled on two well-delimited facies zones, with mean values of 2 cm and 6.5 cm, respectively, implying aggradation of both the halite pan and the halite nucleus facies in this salar, with aggradation rates greater atop the halite nucleus facies association. We observe an annual acceleration approximately between September and March each year, especially well expressed at salar that have high deformation rate (ISLA1, Figure 2h) that could be the evidence of a seasonal effect. PAJ1 is located in the northern part of the salar de Pajonales (Figure 2f) and show a similar linear displacement with respect to ISL2, with a cumulative displacement of 2 cm in almost 5 years. However, PAJ2, atop a zone characterised by sedimentary features indicative of local dissolution (saline pan separated by numerous pools and ponds), shows a clear signal subject to a rapid negative displacement along the satellite LOS direction during the first trimester of 2004, for a duration of almost one year. Note that after 2006, the signal follows again a similar deformation trend

comparable with other areas (PAJ1), and also AMA, located on the salar de Amarga, 50 km distant, south east from Pajonales (Figure 2d, f).

5.3 Deformation signal versus ground composition

To identify the general good agreement between InSAR observation and local geology we further compare profiles sampled across both the InSAR dataset and optical images acquired by the Landsat satellite in 2000 (Figure 3a-b). We employ the Landsat band 7 (mid-IR), which is sensitive to soil moisture and thus, provides contrasted information about the intensity, often critical in salt-rich areas. We first found that the areas with weaker deformation signal (see ISLA2, Figure 2a) correspond to higher intensity values with the optical sensor and geologically to the marginal facies. Second, the areas with stronger deformation signals (see ISLA1, Figure 2a) have lower intensity values, that

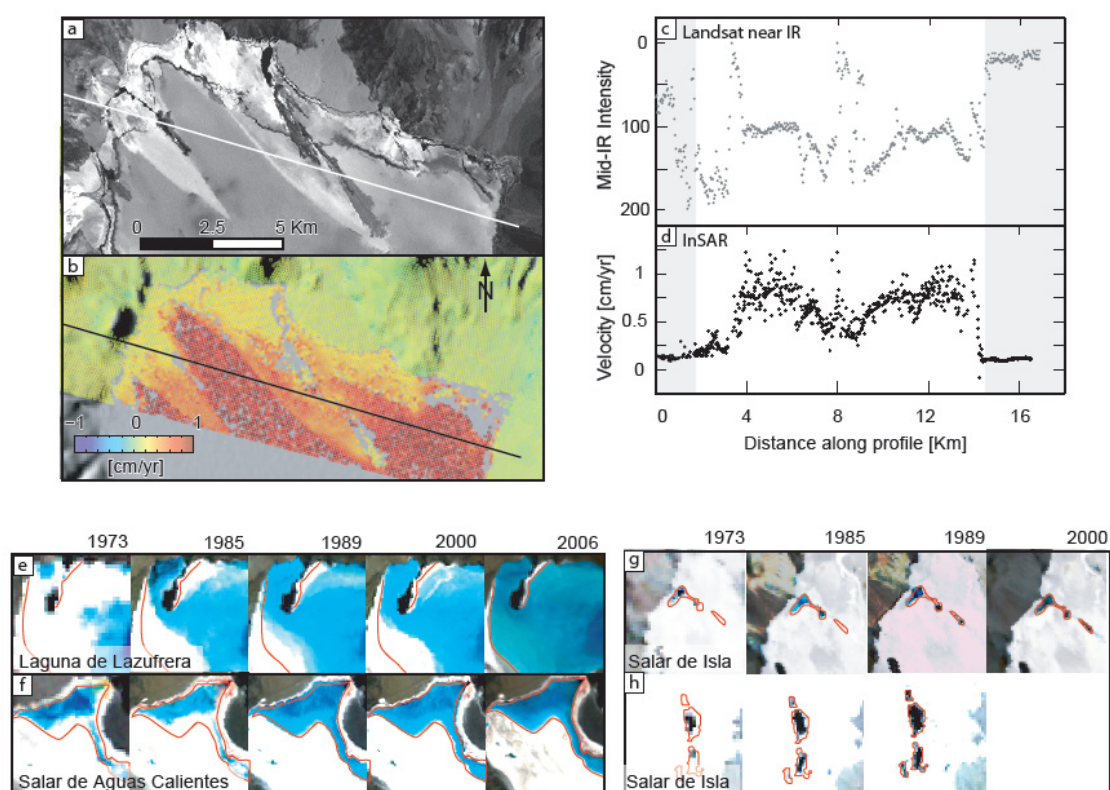


Figure 3. Profiles between InSAR deformation and Landsat intensity images. a) Band 7 in mid-IR taken in 2000, b) InSAR dataset (2003-2008). Profile across the c) Landsat image and d) the InSAR dataset. Note the good agreement between both signals. Lake

level time series using Landsat images (band 321), as on 23/03/1973, 25/01/1985, 27/10/1989, 03/11/2000 and 21/12/2006 focused on perennial lakes, at e) Laguna de Lazufre, f) salar de Aguas Calientes, g), h) at two locations at salar de Isla. The red perimeters is the lake contours as in 2006, note the continuous increase of the lake perimeters since 1973.

corresponds to the halite nucleus where salt typically precipitate by capillarity from shallow groundwater bodies. Profiles across both InSAR velocity map and Landsat intensity images show that signals are in good agreement (Figure 3c-d), where the maximum uplift matches with halite-rich soils, prone to faster salt accretion. To confirm likely hydrological drivers to the varying rates of deformation within and between salars phenomena we also compared our sedimentological/deformation results with published chemical analysis of surface waters, from both water income and laguna locations, that were systematically sampled across the Andes in 1991 (Risacher and Fritz, 1991; Risacher et al., 2009). Although there are no pore water samples in the nucleus facies in the salars under study, hydrogeochemistry samples from the salar edges confirms that the salar with the highest deformation rate of all salar observed, Salar de la Isla, also contains waters with the highest salinity in central Andes. Its maximum salinity is 330g/l, significantly more than at Pajonales (247 g/l) and at Agua Amarga (197 g/l), hence, it is more prone to faster salt precipitation and associated ground deformation.

5.4 Discussion & conclusion

In this study, we present a detailed analysis on salar deformations using InSAR observations, geological information and chemical data in the Western Cordillera of Northern Chile. We show that all salars observed are actively deforming. Our analysis demonstrates a strong intra- and inter-salar association between saline facies distribution and rates of rise or fall of the salar surface.

Although our results strongly suggest that the deformation (aggradation) observed in the salars is directly related to levels of salt precipitation and salt crust thickening, other mechanisms may be contributing locally to the deformation, such as hygroscopic and salt associated expansion of clay soils in regions of groundwater inflow within the salt basin (Gabriel, 1989; Ewing et al., 2006). However, in dry salars, such as the three we studied in detail, there is typically a lack of near-surface clay beds within the halite-encrusted regions. That is, clay is not preserved as “soil” layers in sufficient a volume to explain the observed rises in the ground surface. The observed correlations in ground displacement, sediment/halite facies variations and inferred salinity suggest that our approach, in tying responses in ground surface elevation to varying intensities of halite growth/dissolution mechanisms within and between salars, is viable.

Our observations are taken over a short period of time (a few years) in the salars’ depositional histories. However, a second InSAR dataset using ERS satellite was processed (same as Ruch et al., 2009), which combined with ENVISAT data shows a similar linear deformation time series over more than 10 years (see Auxilliary material), between 1995 to 2008 that was here not detailed because of the coverage limitation of this specific scene.

If a constant deformation (aggradation) rate of $>1\text{cm/year}$ (as observed at Salar de la Isla) continued over a century or more, then the precipitation of halite in the nucleus facies should have induced a height differential of around 1 m/century compared to the aggradation rate of the marginal facies. This is not the case, field observation at Isla and at other salars across the Altiplano indicate that only few tens of centimetres separate the surfaces of the halite nucleus and the margin facies associations, indicating likely variation in the salar dynamics in the past. Transient strong rain or snowfall events on time scales greater than our few years of observation must influence the heights of differentials across the various salar surfaces (Ortlieb, 1985). Alternatively, a continuous

increase of the annual incoming groundwater may accelerate salt crystallization by capillarity. A regional diminution of the permafrost elevation induced by global warming is observed since decades in the Andes (Trombotto and Borzetta, 2009). The resulting increase of the groundwater supply may feeds salar water tables that allows in turn faster salt precipitation. To test this hypothesis, we analysed the evolution of the salar surface using Landsat images available from 1973 to the 2006 acquired during the summer period and observed a continuous increase of the perennial lake dimensions at the salar surface (Figure 3e-f). Both long term (Landsat) and short term (InSAR) time series may explain the deformation rate increase in a yearly and a decennially based activity.

The degree of solute cycling in both the nucleus and pan halites over the longer time frames associated with the halite infill of a drainage sump in an endoreic salar depression has significant implications in terms of: 1) Recognition of hydrologic stability/climatic variability preserved in the infill beds as variable salt signatures. 2) Identification of regions of likely concentration of particular solute components in salar pore brines, such as lithium and boron. The fact that salar surfaces are aggrading at different rates, both within and between salars, has direct geohydrologic and indirect long-term climatic implications.

Water reserve quantification is matter of serious concerns in the central Andes, both for human water supply and also for mining company needs during mineral extraction processes. Use of InSAR monitoring of salar surfaces may help define water budgets within and between salar depressions.

Conclusion and outlook

In this study, we analyse the spatiotemporal evolution of the Lazufre volcano deformation detected by InSAR and provide a new overview of the deformation since its detection in 1997 within its geological context. The deformation is still active after 13 years, and we found that the displacement rate is even progressively increasing. A second small-scale deformation affecting the Lastarria volcano started around 2000 and suggests a possible relationship between the two neighbouring systems. After comparing InSAR data with observations of the volcanic structures, we propose that both independent deformations are the surface expression of a long-lived magmatic system evolving at depth, influenced by constant regional stress activity since the Pleistocene.

Although the present lack of geophysical and geological data in this area does not allow us to construct more realistic models, ongoing ground truth studies at Lazufre will bring additional data to expand such models in the near future.

In the last few years, InSAR time series have provided high-resolution information about multi-scale deformations (10^2 - 10^{-1} km²) that were not previously detectable with standard interferometry. This advance allows us to identify, for instance, flank movements at Lastarria and clear deformation in salars, which, when combined with geological analysis, permit us to better understand the active mechanisms. Although this advanced InSAR technique provides a great amount of new, detailed, full-resolution data on ground deformations, only a small percentage of it has been exploited to date at volcanoes or elsewhere. Future studies integrating full InSAR datasets with complementary geological observations will allow for better understanding of volcanic hazards and associated processes elsewhere.

References

- Acocella, V., T. Korme, F. Salvini and R. Funicello, 2002. Elliptic calderas in the Ethiopian Rift: control of pre-existing structures. *Journal of Volcanology and Geothermal Research*, 119: 189-203.
- Aizawa, K., Y. Ogawa, T. Ishido, 2009. Groundwater flow and hydrothermal systems within volcanic edifices: Delineation by electric self-potential and magnetotellurics, *Journal of Geophysical Research*, 114, doi:10.1029/2008JB005910.
- Alonso, R., T.E. Jordan, K.T. Tabbutt, D.S. Vandervoort, 1991. Giant evaporite belts of the Neogene Central Andes, *Geology*, 19, 401-404.
- Ambrose, S.H., 1998. Late Pleistocene human population bottlenecks, volcanic winter, and differentiation of modern humans, *Journal of Human Evolution*, 34(6): 623-651.
- Amelung, F., S. Jonsson, H. Zebker and P. Segall, 2000. Widespread uplift and "trapdoor" faulting on Galapagos volcanoes observed with radar interferometry, *Nature*, 407(6807): 993-998.
- Anderson, E.M., 1951. *The Dynamics of Faulting*, Oliver and Boyd, Edinburgh.
- Annen, C., 2009. From plutons to magma chambers: Thermal constraints on the accumulation of eruptible silicic magma in the upper crust, *Earth and Planetary Science Letters*, 284, 409-416.
- Assumpção, M. & M. Araujo, 1993. Effect of the Altiplano-Puna plateau, South America, on the regional intraplate stresses. *Tectonophysics*, 221: 475-496.
- Battaglia, M., C. Troise, F. Obrizzo, F. Pingue and G. De Natale, 2006. Evidence for fluid migration as the source of deformation at Campi Flegrei caldera (Italy). *Geophysical Research Letters*, 33 (L01307): doi: 10.1029/2005GL024904.
- Bautista, B.C., M.L.P. Bautista, R.S. Stein, E.S. Barcelona, R.S. Punongbayan, E.P. Laguerta, A.R. Rasdas, G. Ambubuyog, E.Q. Amin, 1996. Relationship of regional and local structures to Mount Pinatubo activity, in *Fire and mud; eruptions and lahars of Mount Pinatubo, Philippines*, University of Washington Press, United States, Quezon City, Philippines.

- Berardino, P., G. Fornaro, R. Lanari, E. Sansosti, 2002. A new algorithm for surface deformation monitoring based on small baseline differential SAR Interferograms, *IEEE Transactions on Geoscience and Remote Sensing*, 40 (11), 2,375-2,383.
- Betancourt, J. L., C. Latorre, J.A. Rech, J. Quade, K.A. Rylander, 2000. A 22,000-Year Record of Monsoonal Precipitation from Northern Chile's Atacama Desert, *Science*, 289, 1542.
- Bonini, M., 2008. Elliptical mud volcano caldera as stress indicator in an active compressional setting (Nirano, Pede Apennine margin, northern Italy), *Geology*, 36(2): 131-134.
- Bosworth, W., K. Burke and M. Strecker, 2003. Effect of stress fields on magma chamber stability and the formation of collapse calderas, *Tectonics*, 22(1042).
- Bürgmann, R., P. Rosen and E. Fielding, 2000. Synthetic aperture radar interferometry to measure Earth's surface topography and its deformation, *Annual Reviews of Earth and Planetary Sciences*, 28: 169-209.
- Casu, F., M. Manzo, R. Lanari, 2006. A Quantitative Assessment of the SBAS Algorithm Performance for Surface Deformation Retrieval from DInSAR Data, *Remote Sensing of Environment*, 102, 195-210.
- Chang, W.L., R.B. Smith, C. Wicks, J.M. Farrell, C.M. Puskas, 2007. Accelerated uplift and magmatic intrusion of the Yellowstone caldera, 2004 to 2006, *Science*, 318, 952-956.
- Chinn, D.S. & B.L. Isacks, 1983. Accurate source depths and focal mechanisms of shallow earthquakes in western South America and in the New Hebrides arc, *Tectonics*, 2(6): 529-563.
- Cole, J.W., D.M. Milner and K.D. Spinks, 2005. Calderas and caldera structures; a review, *Earth-Science Reviews*, 69(1-2): 1-26.
- Coutand, I., A. Chauvin, P.R. Cobbold, and P. Gautier, 2001. Style and history of Andean deformation, Puna plateau, Northwestern Argentina, *Tectonics*, 20(2): 210-234.
- De Silva, S. & P.W. Francis, 1991. *Volcanoes of the Central Andes*, Berlin, Springer-Verlag: 216pp.
- Dieterich, J. & R. Decker, 1975. Finite element modeling of surface deformation associated with volcanism, *J. Geophys. Res.*, 80 (29): 4094-4102.

- Feigl, K.L., J. Gasperi, F. Sigmundsson and A. Rigo, 2000. Crustal deformation near Hengill Volcano, Iceland 1993-1998; coupling between magmatic activity and faulting inferred from elastic modeling of satellite radar interferograms, *Journal of Geophysical Research*, 105(11): 25,655-25,670.
- Fiske, R.S., & E.D. Jackson, 1972, Orientation and growth of Hawaiian volcanic rifts: the effect of regional structure and gravitational stresses: Proc. Royal Society of London, v. 329, p. 299-326.
- Francis, P.W., S.L. de Silva, P.J. Mouginiis-Mark and S. Self, 1989. Large diameter volcanic spatter rings; mechanisms of origin and significance for planetary studies, Abstracts. *Lunar and Planetary Science Conference*, Houston, TX, United States, pp. 307-308.
- Froger, J.L., D. Remy, S. Bonvalot, and D. Legrand, 2007. Two scales of inflation at Lastarria-Cordon del Azufre volcanic complex, central Andes, revealed from ASAR-ENVISAT interferometric data, *Earth and Planetary Science Letters*, 255 (1-2), 148-163.
- Gander, W., G.H. Golub and R. Strebler, 1994. *Least-Squares Fitting of Circles and Ellipses*, BIT Numerical Mathematics, Springer.
- Garleff, K. & H. Stingl, 1986. Geomorphologische Aspekte aktuellen und vorzeitlichen Permafrostes in Argentinien. *Zentralblattes für Geologie und Paläontologie*, 1(9/10), 1367-1374.
- Gottsmann, J., G. Berrino, H. Rymer and J.G. Williams, 2003. Hazard assessment during caldera unrest at the Campi Flegrei, Italy; a contribution from gravity-height gradients. *Earth and Planetary Science Letters*, 211(3-4): 295-309.
- Hanssen, R., 2001. *Radar Interferometry data interpretation and data analysis*, Kluwer academic publishers, Dordrecht, 308 pp.
- Holohan, E.P., V.R. Troll, T.R. Walter, S. Munn, S. McDonnell, Z.K. Shipton, 2005. Elliptical calderas in active tectonic settings: An experimental approach. *Journal of Volcanology and Geothermal Research*, 144: 119-136.
- Hill, D.P., M.J.S. Johnston, J.O. Langbein, and R. Bilham, 1995. Response of Long Valley Caldera to the Mw=7.3 Landers, California, earthquake., *Journal of Geophysical Research*, 100 (7), 12,985-13,005.
- Hill, D.P., F. Pollitz, and C. Newhall, 2002. Earthquake-volcano interactions, *Physics Today*, 55 (11), 41-47.

- Hurwitz, S., L. Christiansen and P.A. Hsieh, 2007. Hydrothermal fluid flow and deformation in large calderas: Inferences from numerical simulations. *Journal of Geophysical Research*, 112(B02206): doi:10.1029/2006JB004689.
- Jellinek, A.M., & D.J. DePaolo, 2003. A model for the origin of large silicic magma chambers: precursors of caldera-forming eruption, *Bulletin of Volcanology*, 65, 363-381.
- Kirkpatrick, S., C.D. Gelatt Jr, and M. P. Vecchi, 1983. Optimization by Simulated Annealing, *Science*, 220, No. 4598, 671-680.
- Lipman, P.W., 1997. Subsidence of ash-flow calderas: relation to caldera size and magma-chamber geometry, *Bulletin of Volcanology*, 59(3): 198-218.
- Lipman, P.W., 2000. Calderas, *Encyclopedia of volcanoes*. Academic Press, San Diego, CA, United States.
- Lu, Z., T. Masterlark, D. Dzurisin, R. Rykhus and C. Wicks, 2000. Magma supply dynamics at Westdahl Volcano, Alaska, modeled from satellite radar interferometry, *Geophysical Research Letters*, 27(11): 1567-1670.
- Lu, Z., T. Masterlark, D. Dzurisin and C. Wicks, 2002a. Subsidence at Kiska Volcano, western Aleutians, detected by satellite radar interferometry, *Geophysical Research Letters*, 29(10.1029/2002GL014948).
- Lu, Z., J.A. Power, V.S. McConnell, C. Wicks and D. Dzurisin, 2002b. Pre-eruptive inflation and surface interferometric coherence characteristics revealed by satellite radar interferometry at Makushin Volcano, Alaska; 1993-2000, *Journal of Geophysical Research*, 107(10.1029/2001JB000970).
- Lu, Z., C. Wicks, D. Dzurisin, J. A. Power, S. C. Moran, and W. Thatcher, 2002c. Magmatic inflation at a dormant stratovolcano; 1996-1998 activity at Mount Peulik Volcano, Alaska, revealed by satellite radar interferometry, *Journal of Geophysical Research*, 107(10.1029/2001JB000471).
- Lundgren, P. & Z. Lu, 2006. Inflation model of Uzon caldera, Kamchatka, constrained by satellite radar interferometry observations, *Geophysical Research Letters*, 33(L06301): doi: 10.1029/2005GL025181.
- Maerten, F., P. Resor, D. Pollard and L. Maerten, 2005. Inverting for slip on three-dimensional fault surfaces using angular dislocations, *Bulletin of the Seismological Society of America*, 95(5): 1654-1665.
- Manconi, A., T.R. Walter, and F. Amelung, 2007. Effects of mechanical layering on volcano deformation, *Geophysical Journal International*, 170, 952-958.

- Manga, M. & E. Brodsky, 2006. Seismic triggering of eruptions in the far field; volcanoes and geysers, *Annual Review of Earth and Planetary Sciences* (34), 263-291.
- Marsh, B.D., 2000. Magma chambers, *Encyclopedia of volcanoes*. Academic Press, San Diego, CA, United States.
- Massonet, D. & K.L. Feigl, 1998. Radar interferometry and its applications to changes in the Earth's surface, *Review of Geophysics*, 36, 441-500.
- Masterlark, T. & Z. Lu, 2004. Transient volcano deformation sources imaged with interferometric synthetic aperture radar; application to Seguam Island, Alaska, *Journal of Geophysical Research*, 109(10.1029/2003JB002568).
- McLeod, P. & S. Tait, 1999. The growth of dykes from magma chambers, *Journal of Volcanology and Geothermal Research*, 92, 231-245.
- McTigue, D.F., 1987. Elastic stress and deformation near a finite spherical magma body: Resolution of the point source paradox, *Journal of Geophysical Research*, 92, 12,931-12,940.
- Meijer, P.T., R. Govers and M.J.R. Wortel, 1997. Forces controlling the present-day state of stress in the Andes, *Earth and Planetary Science Letters*, 148: 157-170.
- Nakamura, K., 1977a. Volcanoes as possible indicators of tectonic stress orientation - principle and proposal, *Journal of Volcanology and Geothermal Research*, 2, 1-16.
- Naranjo, J., 1985. Sulphur flows at Lastarria Volcano in the North Chilean Andes, *Nature*, 313(6005): 778-780.
- Naranjo, J. & P. Francis, 1987. High velocity debris avalanche at Lastarria Volcano in the North Chilean Andes, *Bulletin of Volcanology*, 49 (2), 509-514.
- Naranjo, J., 1992. Chemistry and petrological evolution of the Lastarria volcanic complex in the North Chilean Andes. *Geological Magazine*, 129(6): 723-740.
- Naranjo, J. & P. Cornejo, 1992. Hoja Salar de la Isla, escala 1:250.000.
- Newhall, C. & D. Dzurisin, 1988. Historical unrest at large calderas of the world. *USGS Bulletin*, 1855: 1108.
- Newman, A.V., T.H. Dixon and N. Gourmelen, 2006. A four-dimensional viscoelastic deformation model for Long Valley Caldera, California, between 1995 and 2000. *Journal of Volcanology and Geothermal Research*, 150: 244-269.
- Núñez, L., M. Grosjean and I. Cartajena, 2002. Human Occupations and Climate Change in the Puna de Atacama, Chile, *Science* 298, 821.

- Oncken, O., D. Hindle, J. Kley, K. Elger, P. Victor, K. Schemmann, 2006. Deformation of the Central Andean Upper Plate System - Facts, Fiction, and Constraints for Plateau Models, in: O. Oncken, G. Chong, G. Franz, P. Giese, H.J. Götze, V. Ramos, M. Strecker, and P. Wigger (eds.): *The Andes. Active subduction orogeny*, Springer, Berlin, p. 3-27.
- Okada, Y., 1985. Surface deformation due to shear and tensile faults in a half-space, *Bulletin of the Seismology Society of America*, 75, 1135-1154.
- Ort, M.H., B.L. Coira and M.M. Mazzoni, 1996. Generation of a crust-mantle magma mixture; magma sources and contamination at Cerro Panizos, central Andes. *Contributions to Mineralogy and Petrology*, 123(3): 308-322.
- Ortieb, L., 1995. El Nino event and rainfall episodes in the Atacama desert: the record of the last two centuries. *Bulletin de l' Institut francais des études Andines*, 24 (3), 519-537.
- Paulsen, T.S. & T.J. Wilson, 2007. Elongate summit calderas as Neogene paleostress indicators in Antarctica. Online Proceedings of the 10th ISAES, USGS Open-File Report 2007-1047, Short Research Paper 072.
- Pedersen, R. & F. Sigmundsson, 2004. InSAR based sill model links spatially offset area of deformation and seismicity for the 1994 unrest episode at Ejyafjallajokull Volcano, Iceland, *Geophysical Research Letters*, 31(10.1029/2004GL020368).
- Pritchard, M.E. & M. Simons, 2002. A satellite geodetic survey of large-scale deformation of volcanic centres in the central Andes, *Nature*, 418 (6894), 167-171.
- Pritchard, M.E. & M. Simons, 2004. An InSAR-based survey of volcanic deformation in the southern Andes, *G3*, 5 (2), 1-42.
- Reigber, A. & J. Moreira, 1997. Phase unwrapping by fusion of local and global methods. Proceedings of IGARSS'97: 869-871.
- Richards, J.P. & M. Villeneuve, 2002. Characteristics of late Cenozoic volcanism along the Archibarca lineament from Cerro Llullaillaco to Corrida de Cori, northwest Argentina, *Journal of Volcanology and Geothermal Research*, 116, 161-200.
- Riller, U. & O. Oncken, 2003. Growth of the central Andean plateau by tectonic segmentation is controlled by the gradient in crustal shortening. *Journal of Geology*, 111(3): 367-384.
- Risacher F, H. Alonso, C. Salazar, 2003. The origin of brines and salts in Chilean salars: a hydrochemical review, *Earth-Science Reviews*, 63, 249-293.

- Risacher, F. & B. Fritz, 1991b. Geochemistry of Bolivian salars, Lipez, southern Altiplano. Origin of solutes and brine evolution. *Geochimica et Cosmochimica Acta* 55, 687–705.
- Ruch, J., J. Anderssohn, T.R. Walter, and M. Motagh, 2008. Caldera-scale inflation of the Lazufre volcanic area, South America: Evidence from InSAR, *Journal of Volcanology and Geothermal Research*, 174 (4), 337-344.
- Ryan, M.P., 1987. Neutral buoyancy and the mechanical evolution of magmatic systems, *Magmatic Processes: Physicochemical Principles*. *Geochemical Society*, pp. 259–287.
- Savin, G.N., *Stress Concentration around Holes*, Pergamon Press, New York, 430pp, 1961.
- Schilling, F.R., R.B. Trumbull, H. Brasse, C. Haberland, G. Asch, D. Bruhn, K. Mai, V. Haak, P. Giese, M. Muñoz, J. Ramelow, A. Rietbrock, E. Ricaldi, T. Vietor, 2006. Partial Melting in the Central Andean Crust: a Review of Geophysical, Petrophysical, and Petrologic Evidence. In: O. Oncken et al. (Editors), *The Andes. Active Subduction Orogeny*. Springer, pp. 459-474.
- Schurr, B., G. Asch, A. Rietbrock, R. Kind, M. Pardo, B. Heit, T. Monfret, 1999. Seismicity and average velocities beneath the Argentine Puna plateau. *Geophysical Research Letters*, 26(19): 3025-3028.
- Siebert, L. & T. Simkin, 2002-. *Volcanoes of the World: an Illustrated Catalog of Holocene Volcanoes and their Eruptions*. Smithsonian Institution, Global Volcanism Program, Digital Information Series, GVP-3, (<http://www.volcano.si.edu/world/>).
- Stanton, J.M., 2001. Galton, Pearson and the Peas: a brief history of linear regression for statistic instructors, *Journal of Statistics Education*, 9 (3).
- Takada, A., 1994. The influence of regional stress and magmatic input on styles of monogenetic and polygenetic volcanism, *Journal of Geophysical Research*, 99:13563-13573.
- Tarantola, A., 1987. *Inverse problem theory, method for data fitting and model parameter estimation*. Elsevier, pp. 613.
- Thomas, A.L., 1993. Poly3D: A three-dimensional, polygonal element, displacement discontinuity boundary element computer program with applications to fractures, faults, and cavities in the Earth's crust, pp 110, Stanford University, Stanford, California.

- Tibaldi, A., 1995. Morphology of pyroclastic cones and tectonics, *Journal of Geophysical Research*, 100(B12): 24,521–24,535.
- Tibaldi, A., C. Corazzato and A. Rovida, 2009. Miocene-Quaternary structural evolution of the Uyuni-Atacama region, Andes of Chile and Bolivia, *Tectonophysics*, 471 (1,2), 114-135.
- Tizzani, P., M. Battaglia, G. Zeni, S. Atzori, P. Berardino, R. Lanari, 2008. Uplift and magma intrusion at Long Valley caldera from InSAR and gravity measurements, *Geology*, 37 (1), 63-66.
- Trumbull, R.B, 1999. Evidence for Late Miocene to Recent contamination of arc andesites by crustal melts in the Chilean Andes (25-26°S) and its geodynamic implications, *Journal of South American Earth Sciences*, 12: 135-155.
- Wallmann, P.C., D. Pollard, W. Hildreth, and J.C. Eichelberger, 1990. New structural limits on magma chamber locations at the Valley of ten thousand smokes, Katmai National Park, Alaska, *Geology*, 18(12): 1240-1243.
- Walter, T.R. & F. Amelung, 2007. Volcanic eruptions following $M > 9$ megathrust earthquakes; implications for the Sumatra-Andaman volcanoes. *Geology*, 35(6): 539-542.
- Walter, T.R., 2007. How a tectonic earthquake may wake up volcanoes: Stress transfer during the 1996 earthquake-eruption sequence at the Karymsky Volcanic Group, Kamchatka, *Earth and Planetary Science Letters*, 264, 347-359.
- Wang, H.F., 2000, *Theory of Linear Poroelasticity: with Applications to Geomechanics*, Princeton University Press, Princeton, 287 pp.
- Warren, J.K., 2006. *Evaporites: sediments, resources and hydrocarbons*, Springer Berlin, 1041p.
- Wicks, C., W. Thatcher, D. Dzurisin and J. Svarc, 2006. Uplift, thermal unrest and magma intrusion at Yellowstone caldera. *Nature*, 440: 72-75.
- Williams, H., 1941. *Calderas and their origin*. University of California Publications in Geological Sciences, 25(6): 239-346.
- Williams, C.A. & G. Wadge, 1998. The Effects of Topography on Magma Chamber Deformation Models: Application to Mount Etna and Radar Interferometry, *Geophysics Research Letters*, 25, 1549-1552.
- Yun, S., P. Segall and H. Zebker, 2006. Constraints on magma chamber geometry at Sierra Negra Volcano, Galapagos Islands, based on InSAR observations, *Journal of Volcanology and Geothermal Research*, 150: 232-243.

CURRICULUM VITAE

Dipl. Geologist **Joël Ruch**

Dipartimento di Scienze Geologiche
Universita' Roma Tre
Lungo S.L. Murialdo
00146 Roma, Italy
Tel: 0039 345 3916204
e-mail: jruch@uniroma3.it



Born in Geneva (Switzerland)
Swiss citizenship, resident in Roma (Italy)

ACADEMIC CARREER

Since June 2009 Post-doc position at the Dipartimento di Scienze Geologiche, Universita Roma Tre, Italy. Topic: Volcano deformation and tectonic activity.

Since April 2006 PhD Candidate, University of Potsdam (Germany), Department of Natural Disasters and Early Warning System of the Helmholtz Centre of Geosciences, GFZ Potsdam (Germany). Topic: Volcano deformation and structural analysis in central Andes.

July 2004 Post-graduate certificate CERG (Centre of Study and management in Geological Risks), University of Geneva (Switzerland).

June 2004 Master in Geology, University of Geneva (Switzerland), Science Faculty, Department of Geology, supervisor Prof. M. Dungan (5.5/6).

June 2002 Bachelor in Earth Sciences, University of Geneva (5/6).

WORK EXPERIENCE

On volcanoes

2008 (Jan & March) "Lazufre project" (central Andes). Installation of seismic and GPS networks in the Lazufre volcanic area. Installation test of a multi-parameter station at Lastarria volcano (gravimeter, thermocouples at HT fumaroles, P sensor) to assess daily hydrothermal activity variations.

2007 (Feb) Installation of two GPS networks in North Chile at Isluga and Lastarria volcanoes coupled with microgravity measurements to assess relationship between fault activation and volcanic activity after earthquakes.

2006-07(Dec.) Project in Dominica. Installation of a continuous P/T sensors at Boiling Lake. Microgravity network installation in South Dominica with Dr. N. Fournier, (Seismic Research Centre, Trinidad, West Indies).

2005 (February-April) Internship at the **Seismic Research Unit** (West Indies). Field assistance for GPS network installation, gas measurements at St Lucia. Project on Volcanic risk assessments in Saint Lucia Island using GIS, with Dr. N. Fournier.

2005 (November) Field assistance in North Thailand involved in a structural and geological mapping project with the **University of Lausanne** (Switzerland) with Dr. O. Ferrari.

2003 (Jan.-March) **Goma Volcano Observatory** (RD Congo). Field assistance with the GVO (GPS and gas measurements, mapping). Project about the evolution of the communication during the 2002 Nyiragongo evolution. Project with J. Durieux (UNOPS), Dr. D. Tedesco (Naples University) and Dr. J.-C. Komorowski (IPGP, Paris).

Elsewhere

2007 (Dec.) Participation to the **GFZ Task Force** mission after the M7.8 Tocopilla earthquake in North Chile, installation of a GPS network to analyse post seismic slip.

2005 (Oct.-Febr.) Internship at **UN-ISDR** (International Strategy for Disaster Reduction) in Geneva & coordinator assistant for the WCDR Conference, Kobe, Japan.

2005 **LaREH** (Laboratory of Research on Human Settlements, IAUG, Uni-Geneva) scientific collaborator and teaching for geological risk assessments, with Prof. R. Mariani.

2003-2004 Assistant position at the University of Geneva for the **CERG** courses (Centre of Study and management in Geological Risks), University of Geneva (Switzerland) with Prof. J.-J. Wagner. Teaching geophysics.

LANGUAGE

French: Native.

English: Fluent speaking and writing.

Italian: Fluent speaking, reading.

German: Good speaking.

Spanish: basic level

COMPUTER SKILLS

Operative Systems: Windows, Linux

Software: Office (Word, Excel, Power Point), Email and Internet.

Technical Softwares: ArcGIS 9.2, Matlab, Poly3D (BEM), ENVI, Davis (PIV), GID, Surfer.

Graphics Software: Adobe Photoshop, Adobe Illustrator.

PUBLICATIONS (ISI)

J. Ruch, V. Acocella, F. Storti, M. Neri, S. Pepe, G. Solaro and E. Sansosti (2010), Detachment depth revealed by rollover deformation: An integrated approach at Mount Etna, *Geophys. Res. Lett.*, doi:10.1029/2010GL044131, in press.

G. Solaro, V. Acocella, S. Pepe, **J. Ruch**, M. Neri, E. Sansosti (2010). Anatomy of an unstable volcano through InSAR observations from 1994 to 2008: multiple processes affecting flank instability at Mt. Etna, *Journal of Geophysical Research*, in press.

J. Ruch & T.R. Walter (2010). Relationship between current uplift geometry (InSAR) and the structural framework at Lazufre volcanic area, central Andes. *Tectonophysics*, in press.

J. Ruch, Manconi A, Zeni G, Solaro G, Pepe A, Walter TR, Lanari R (2009). Different deformation scales and stress field change in the Lazufre volcanic area, Central Andes. *Geophysical Research Letters*, 36, L22303, doi:10.1029/2009GL041276.

J. Ruch, J. Anderssohn, T.R. Walter, M. Motagh (2008) Caldera-scale inflation of the Lazufre volcanic area, South America, evidenced by InSAR. *Journal of Volcanology and Geothermal Research*, 174 (4), 337-344, doi:10.1016/j.jvolgeores.2008.03.009.

J. Ruch & D. Tedesco (2003). One year after the Nyiragongo volcano alert: evolution of the communication between Goma inhabitants (populations), scientists and local authorities. *Acta Vulcanologica*, 14 (1-2), pp. 101-108.

BOOK CHAPTER

J. Ruch, & D. Tedesco (2005). One year after the Nyiragongo volcano alert: evolution of the communication between Goma inhabitants (populations), scientists and local authorities. *Known Risk*, United Nations press, p. 376.

PUBLICATIONS (NON ISI) & INTERNATIONAL CONFERENCES

J. Ruch, A. Manconi, G. Diringler, T.R. Walter. Flank stability analysis at Lastarria volcano (northern Chile): insights from rock failure criterion and InSAR observations. EGU meeting 2010, Geophysical Research Abstracts, Vienna (*poster*).

J. Ruch, A. Manconi, G. Zeni, G. Solaro, A. Pepe, M. Shirzaei, T.R. Walter, R. Lanari. Stress transfer in the Lazufre volcanic area, central Andes. EGU meeting 2010, Geophysical Research Abstracts, Vienna (*oral presentation*).

J. Ruch, J.K., Warren, F. Risacher, T. Walter, R. Lanari (2009). Continuous salar deformations in the Puna plateau (central Andes): insights from InSAR data and ground composition. Fringe Meeting, Dec. 2009, Frascati, Roma, Italy (*poster*).

J. Ruch & T.R. Walter. Elliptical deformation as a possible stress indicator (Lazufre volcanic area, Central Andes) investigated through InSAR and GIS studies. EGU meeting 2009, Geophysical Research Abstracts, Vienna (*oral presentation*).

J. Ruch, A. Manconi, G. Zeni, G. Solaro, A. Pepe, T.R. Walter, R. Lanari. Volcano deformation revealed by DInSAR measurements and stress transfer in the Lazufre area, Central Andes, EGU meeting 2009, Geophysical Research Abstracts, Vienna (*poster*).

J. Ruch, T.R. Walter, R. Lanari (2008) Different time scale deformations observed at the Lazufre volcanic area (South America) revealed by InSAR analysis IAVCEI General assembly, Reykjavik, Iceland, 21 August 2008 (*poster*).

J. Ruch & T.R. Walter (2008) Local stress change on the Lastarria volcanic complex (South America) after a regional volcanic inflation: Insights from InSAR and structural analysis. VMSG meeting, Dublin, 4 January 2008 (*oral presentation*).

J. Ruch & T.R. Walter (2008) Large volcanic inflation at Lazufre (North Chile) evidenced by InSAR and structural analysis. Geologische Vereinigung International workshop, Bremen, 4 October 2007 (*oral presentation*).

J. Ruch, T.R. Walter, J. Anderssohn, M. Motagh (2007) Volcanic deformation in Chile after a large subduction earthquake: lessons learned from Cordòn del Azufre volcanic area, 25°S- 68°W EGU meeting, Geophysical Research Abstracts, Vienna (*poster*).

J. Ruch, T.R. Walter, J. Anderssohn (2006) Volcanic deformation in Chile after a large subduction earthquake: lessons learned from Cordòn Lazufre volcanic area, 25°S-68°W. Geologische Vereinigung International Workshop, Potsdam, 26 September 2006 (*poster*).

J. Ruch & N. Fournier (2005). Volcanic risk assessments in Saint Lucia island, Lesser Antilles: quantified evaluation of the affected population and estimation of the economical losses. Cities on Volcanoes IV, Quito, Ecuador (*poster*).

J. Ruch, & D. Tedesco (2005) in: One year after the Nyiragongo volcano alert: evolution of the communication between Goma inhabitants (populations), scientists and local authorities. *Known Risk*, United Nations press, p. 376.

J. Ruch, J.J Wagner (2004), Gestion de crise et communication durant l'éruption du volcan Nyiragongo (17 janvier 2002) en République Démocratique du Congo, CERG master report, Sciences de la Terre, Université de Genève.

J. Ruch, (2002) Multidisciplinary studies about the monogenetic Resago volcano (36.27°S), Annual Meeting, VMSG, Edinburgh, UK (*poster*).
